



LAWRENCE
LIVERMORE
NATIONAL
LABORATORY

LLNL-TR-410158

LIFE Materials: Phase Formation and Transformations in Transmutation Fuel Materials for the LIFE Engine Part I - Path Forward Volume 3

P. E. A. Turchi, L. Kaufman, M. Fluss

January 28, 2009

Disclaimer

This document was prepared as an account of work sponsored by an agency of the United States government. Neither the United States government nor Lawrence Livermore National Security, LLC, nor any of their employees makes any warranty, expressed or implied, or assumes any legal liability or responsibility for the accuracy, completeness, or usefulness of any information, apparatus, product, or process disclosed, or represents that its use would not infringe privately owned rights. Reference herein to any specific commercial product, process, or service by trade name, trademark, manufacturer, or otherwise does not necessarily constitute or imply its endorsement, recommendation, or favoring by the United States government or Lawrence Livermore National Security, LLC. The views and opinions of authors expressed herein do not necessarily state or reflect those of the United States government or Lawrence Livermore National Security, LLC, and shall not be used for advertising or product endorsement purposes.

This work performed under the auspices of the U.S. Department of Energy by Lawrence Livermore National Laboratory under Contract DE-AC52-07NA27344.

LIFE Materials:

**Phase Formation and Transformations in
Transmutation Fuel Materials for the LIFE Engine
Part I – Path Forward**

Volume 3

Patrice E. A. Turchi

**Physical and Life Sciences Directorate
Lawrence Livermore National Laboratory
7000 East Avenue
Livermore, California 94550**
Phone: (925) 422-9925; Email: turchi1@llnl.gov

Larry Kaufman

**CALPHAD Inc.
140 Clark Road
Brookline, Massachusetts 02445-5848**
Phone: (617) 566-7096; E-mail LaryKaufman@rcn.com

Michael J. Fluss

**Physical and Life Sciences Directorate
Lawrence Livermore National Laboratory
7000 East Avenue
Livermore, California 94550**
Phone: (925) 423-6665; E-mail: fluss1@llnl.gov

TABLE OF CONTENTS

LIST OF TABLES.....	3
LIST OF FIGURES.....	4
ACRONYMS AND ABBREVIATIONS.....	7
EXECUTIVE SUMMARY	10
CHAPTER A. INTRODUCTION.....	11
CHAPTER B. APPROACHES TO SOLID ULTRA-HIGH BURN-UP FUEL	14
Tristructural-isotropic (TRISO) Fuels	15
<i>Shortcomings of TRISO Fuel and Research Directions</i>	<i>15</i>
<i>Thermo-mechanical response of PyC.....</i>	<i>17</i>
<i>Fission gas pressure.....</i>	<i>18</i>
<i>CO pressure</i>	<i>18</i>
<i>Kernel migration.....</i>	<i>18</i>
<i>Pd attack</i>	<i>19</i>
<i>Cesium release</i>	<i>19</i>
Inert Matrix (IMF) and Dispersed Fuels	20
<i>Shortcomings of IMF and Research Directions</i>	<i>21</i>
CHAPTER C. WHERE ARE WE TODAY IN THE CONTEXT OF LIFE?	23
TRISO Fuel Option.....	23
<i>Specific Research Directions</i>	<i>23</i>
<i>Kernel.....</i>	<i>24</i>
<i>PyC buffer.....</i>	<i>24</i>
<i>IPyC</i>	<i>25</i>
<i>Ceramic capsule (SiC ZrC...etc).....</i>	<i>25</i>
<i>TRISO systems issues</i>	<i>25</i>
Solid Hollow Core (SHC) Fuel Option.....	25
<i>Specific Research Directions</i>	<i>26</i>
Inert Matrix Fuel (IMF) Option	26
<i>Specific Research Directions</i>	<i>28</i>
CONCLUSIONS.....	29
ACKNOWLEDGMENTS.....	31
BIBLIOGRAPHY.....	32
FIGURES	42
TABLES	35
APPENDIX A. THERMO-CALC AND CALPHAD MODELING	58
References.....	60
APPENDIX B. THERMODYNAMIC DATABASE FOR SOLID FUEL MODELING.....	61
References – Binary Alloys	66
References – Other Binaries of Interest	72
References – Ternaries and Higher-Order Component Alloys.....	76
References – Miscellaneous.....	80

List of Tables

Table I. Partial view of the LIFE engine that shows where the molten salt blanket (in red) is located	35
Table II. Substantial quantities of coated particles have already been fabricated in facilities throughout the world [Vennerri 2005].....	35
Table III. Kernel and TRISO coating specifications in some current applications [General Atomics 2006].....	36
Table IV – Classes of inert matrices that have been proposed as candidates for IMF.	36
Table V – Comparison of fuel service conditions.	37
Table VI – Comparative design characteristics of container-type fuels (MOX and U-20Pu-10Zr metal fuel), and novel combined UMo-PuO ₂ dispersion fuel for fast reactors.....	38
Table VII – Alloy composition (in wt.%), melting and brazing temperatures (T) of potential Zr-based brazing alloys.....	39
Table VIII – Components, granule size, and melting temperature of the U-PuO ₂ fuel.....	39
Table IX – Volume fraction, fuel content, and melting temperature after manufacturing of the combined U-PuO ₂ fuel.....	40
Table X – In-pile tests of prototype fuels with UO ₂	40
Table XI– Summary of the output of the Solid Fuel Working Group on the <i>a priori</i> adequacy of the known options.....	40
Table XII– Challenges facing all solid fuel option.....	41

List of Figures

Figure 1. TRU formed as a function of FIMA, in grams per MTIHM (left) and per GWe-year (right) [Shaw and Latkowski 2008].	42
Figure 2. Partial view of the LIFE engine that shows (in red) where, in the solid fuel option, the fuel is located in the fuel fission blanket	42
Figure 3. Partial view of the LIFE engine that shows where the molten salt blanket (in red) is located	43
Figure 4 – Fission products and gases generated by a DU fuel as a function of burn-up (% FIMA).	43
Figure 5 – Parts of a TRISO particle – a miniature pressure vessel	44
Figure 6 – The base-line fuel anticipated for the South African PBMS reactor. The three coating layers and the buffer layer are designed to be a lifetime coating and encapsulation for the fuel-kernel shown in red. The aggregate fuel is shown in the two left most illustrations.	44
Figure 7 – Photos of the TRISO particles and cylindrical pellet, left, and the carbon prismatic fuel block for the DB-MHR, right	45
Figure 8 – Mechanical forces are shown in a typical TRISO particle.	45
Figure 9 – An example of how the use of ZrC improves TRISO deep-burn performance, left to right: replace SiC with ZrC, use as a getter in the buffer, use as a getter and barrier around the kernel.	46
Figure 10 – Migration of a UO ₂ kernel in a TRISO particle	46
Figure 11 – Schematic representation of the corrosion mechanism of the SiC layer by the FP Pd in a TRISO particle	47
Figure 12 – Pd penetration rate into SiC as a function of the inverse temperature, based on international data.	48
Figure 13 – Photomicrographs of large thru-wall columnar SiC grains and smaller SiC grains produced in UCO fuel.	48
Figure 14 – Examples of IMF fuel pellets. (Left) spinel based IMF with a heterogeneous micro dispersion (<25µm) and (right) spinel with heterogeneous macro-dispersion (>100 µm) of fuel spheres that can be seen at the surface of the pellet.	49

Figure 15 – Examples of cross-sections of a macro-dispersed IMF (left) using microspheres $\sim 100\ \mu\text{m}$ \varnothing of fuel and a micro-dispersed IMF (right) using crushed $<25\ \mu\text{m}$ \varnothing of the same fuel microspheres.49

Figure 16 – Three points are shown in this illustration: (blue) represents successful experience with TRISO fuels achieving FIMA of $\sim 20\%$ using LEU; (green) successful exploratory research with TRISO fuels burning HEU or Pu, or Pu+MA to FIMA of $\sim 70\%$; and (red) represents the goal for achieving ultra-high burn-up (FIMA $>90\%$) for LEU or NEU TRISO fuels in hybrid reactors. While high burn-up is a specific challenge because most of the fuel is FP at EOL, the radiation effects from the large neutron fluence also represents an additional challenge to the materials design.50

Figure 17 – US VHTR and German HTGR fuels operating envelope compared with LIFE requirements. Note that power density, burn-up, and fast-fluence axes are on a log scale.51

Figure 18 – Evolution of fuel components with FIMA (i.e., time or burn-up).....51

Figure 19 – Failure mechanisms and their pathways for standard TRISO particles52

Figure 20 – Main issues that affect the performance of TRISO particle.52

Figure 21 – Schematics of a solid hollow core fuel.....53

Figure 22 – Schematics representation of IMF version proposed for thermal and fast reactors. Impregnation (left), capillary impregnation (middle), and impregnation of a Zr matrix (right).53

Figure 23 – Schematics representation of IMF version originally proposed for thermal reactor. Cross section of fuel element with heterogeneous arrangement of fuel (left), microstructure of UO_2 fuel sample (middle), and microstructure of sample of heterogeneously arranged fuel element with UO_2 in a Zr-based matrix, Zr-6.2Fe-02.5Be (right)54

Figure 24 – Schematics representation of heterogeneous fuel arrangement within the pores of a Zr-based alloy frame. Microstructure of Zr porous matrix fabricated by capillary impregnation from Zr powder (left), Zr granules (middle), and U-PuO₂ dispersion (with PuO₂ located schematically in the pores).....54

Figure 25 – Appearance of the initial components of the combined U-PuO₂ fuel: (a) U-Mo alloy granules, (b) Zr-Fe-Cu alloy matrix granules, and (c) PuO₂ powder manufactured by pyro-chemical method55

Figure 26 – Example of a process-flow sheet of fuel-element fabrication by a capillary-impregnation method55

Figure 27 – U-PuO₂ dispersion combined fuel, in replacement of MOX fuel, and fabrication stages.....56

Figure 28 – Flow chart describing the relations between thermodynamic and kinetic studies and properties and performance of advanced metallic nuclear fuels.....57

Acronyms and Abbreviations

AFCI	Advanced Fuel Cycle Initiative
AGR	Advanced Gas Reactor
BOI	Beginning Of Irradiation
CALPHAD	CALculation of PHAse Diagrams
CSNF	Conventional Spent Nuclear Fuel
DB-MHR	Deep Burn-Modular High-temperature Reactor
DICTRA	Diffusion-Controlled TRAnsformation
dpa	Displacement Per Atom
DSC	Differential Scanning Calorimetry
DTA	Differential Thermal Analysis
DU	Depleted Uranium
FBR	Fast Breeder Reactor
FIMA	Fissions per Initial Metal Atom (a measure of burn-up in nuclear fuel) that corresponds to the number of fissions per initial heavy metal atom, expressed in terms of the proportion of fissions occurring in a population of atoms. The correspondence with specific burn-up (MW.d/tM) is $1\% \text{ FIMA} \approx 9,600 \text{ MW.d/tM}$, and the burn-up fraction is given by $1 \text{ at.\%} \approx 10 \text{ GW.d/tiHM}$.
FG	Fission Gas(es)
FP	Fission Product(s)
GA	General Atomics
Gen-IV	Generation IV
GNEP	Global Nuclear Energy Partnership
HEU	High-Enriched Uranium (usually $\sim 93\%$ ^{235}U)
HTGR	High-Temperature Gas-cooled Reactor
HTR	High-Temperature Reactor (pebble-bed core)

HV	Heavy Metal
HWR	Heavy-Water Reactor
IMF	Inert Matrix Fuel
IPyC	Inner Pyrolytic Carbon coating in a TRISO particle
ITER	International magnetic fusion project, Latin word for “the way”
LEU	Low-Enriched Uranium (<19.9% ²³⁵ U)
LIFE	Laser Inertial Fusion-Fission Energy
LLNL	Lawrence Livermore National Laboratory
LWR	Light-Water Reactor
MA	Minor Actinides
MSR	Molten Salt Reactor
NatU	Natural Uranium
OPyC	Outer Pyrolytic Carbon coating in a TRISO particle
ORNL	Oak Ridge National Laboratory
PISA	Pressure Induced Stress Analysis
PBMR	Pebble Bed Modular Reactor
P-PyC	“Protective” Pyrolytic Carbon coating in a TRISO-P particle
PyC	Pyrolytic Carbon
SiC	Silicon Carbide coating in a TRISO particle
SNM	Spent Nuclear Fuel
TDB	To Be Determined
TEM	Transmission Electron Microscopy
TF	Transmutation Fuel
TRISO	TRI-ISOtropic coated fuel particle design with three materials in coating system (low-density PyC, high-density PyC, and SiC)

TRU	TransUranic
UCO	A mixture of UO ₂ and UC ₂
VHTR	Very High-Temperature Reactor
V&V	Verified & Validated
WGPu	Weapon-Grade Plutonium
YSZ	Yttria Stabilized Zirconia

Executive Summary

The current specifications of the LLNL fusion-fission hybrid proposal, namely LIFE, impose severe constraints on materials, and in particular on the nuclear fissile or fertile nuclear fuel and its immediate environment. This constitutes the focus of the present report with special emphasis on phase formation and phase transformations of the transmutation fuel and their consequences on particle and pebble thermal, chemical, and mechanical integrities. We first review the work that has been done in recent years to improve materials properties under the Gen-IV project, and with in particular applications to HTGR and MSR, and also under GNEP and AFCI in the USA. Our goal is to assess the nuclear fuel options that currently exist together with their issues. Among the options, it is worth mentioning TRISO, IMF, and molten salts. The later option will not be discussed in details since an entire report (Volume 8 – Molten-salt Fuels) is dedicated to it. Then, in a second part, with the specific LIFE specifications in mind, the various fuel options with their most critical issues are revisited with a path forward for each of them in terms of research, both experimental and theoretical. Since LIFE is applicable to very high burn-up of various fuels, distinctions will be made depending on the mission, *i.e.*, energy production or incineration. Finally a few conclusions are drawn in terms of the specific needs for integrated materials modeling and the in depth knowledge on time-evolution thermo-chemistry that controls and drastically affects the performance of the nuclear materials and their immediate environment. Although LIFE demands materials that very likely have not yet been fully optimized, the challenges are not insurmountable, and a well concerted experimental-modeling effort should lead to dramatic advances that should well serve other fission programs such as Gen-IV, GNEP, AFCI as well as the international fusion program, ITER.

Chapter A. Introduction

The LLNL hybrid fusion-fission concept under the acronym LIFE has been proposed to design an engine that can achieve very high burn-up (up to 99% FIMA) of the various fuels: NatU, DU, HEU, SNM, and WGPu, as well as Thorium, thus eliminating the need for reprocessing and minimizing the waste to that of short-lived FP. Hence, the mission envisioned for the LIFE engine falls into 4 categories:

- Burning of DU and NatU to > 97 % burn-up
- Burning of pre-processed LWR SNM to > 97 % burn-up
- Burning of excess WGPu
- Burning of Thorium

In a LIFE engine, there is an imperative to reach high burn-up as shown in Fig. 1 in the case of a DU fuel, where the amount of TRU generated during the life of the engine is plotted as a function of burn-up (% FIMA). For the purpose of storing the minimum amount of TRU waste, compared to conventional SNF, high burn-up beyond 90% must be achieved [Shaw et al. 2008] since for most of the engine life, the fission fuel has a higher concentration of TRU than typical spent LWR fuel.

Thus, this fusion-fission concept requires a research effort on the fundamental science necessary to realize very high burn-up (to achieve lower ratio TRU/energy generated than CSNF) and ultra high burn-up fuel (to have lower mass concentration of TRU than CSNF, which is the repository-relevant metric). What we mean by very-high and ultra-high burn-up is $>50\%$ and $>90\%$ FIMA, respectively, in the original fuel without intervening reprocessing. While such a goal is arguably extraordinarily aggressive with regards to the materials performance of the fuel and its containment, it is not beyond reason. Success will not only reduce the cost of geological storage, but the very concept has intrinsic non-proliferation and safeguard components associated with extended containment of SNM within the reactor system, a clear advantage compared to nuclear fuel cycles that make heavy use of reprocessing and recycling. Moreover, if implemented appropriately, this strategy could extend the reserves of known uranium for millennia, and economically facilitate the effective use of NatU and/or Th in the nuclear fuel cycle.

Various fuel options based on current knowledge of advanced TF for FBRs that are studied in the framework of the Gen-IV and GNEP reactor programs have been proposed, and will be discussed in this development plan. The purpose is not so much, at this early stage, to offer a final solution, since the LIFE specifications are rather unique and still evolving, but instead to provide a critical examination of the technical issues associated with various possible options, with a special emphasis on thermal integrity, phase formation and transformations of TF as a function of burn-up.

The current options that have been considered for fuel form fall into two categories: solid fuels and molten salt fuels, each with their specific issues and challenges. Note that unless defined otherwise, “fuel” and “fuel form” will be referring in the following to nuclear fuel itself and its primary containment.

For solid fuels, based on previous studies carried out under various programs, it is worth mentioning TRISO and IMF, and in the current design of the LIFE engine, the TF should be allowed to circulate inside a spherical-shaped blanket and be exposed at temperatures not exceeding 800 °C, see Fig. 2. For both options the performance criteria and requirements are:

- High fuel density, i.e., high conversion ratio
- Low fuel temperature, at least compatible with LIFE specifications, i.e., <800 oC
- High burn-up, i.e., excellent behavior in a drastic varying chemistry with time
- Accommodation of FG pressure
- Resistance of the cladding to chemical attack of corrosive FP
- High irradiation resistance at the fuel cladding interface, i.e., low damage by FP, and hence low swelling
- Resistance to swelling and mechanical property changes in the fuel cladding and fuel assembly due to radiation displacement damage
- High thermal conductivity (to ensure optimum thermal transport)
- Optimum fuel-cladding contact to maximize thermal transport
- Workability in transients
- Environment-friendly fabrication process, and low fabrication cost
- Production of a suitable wasteform for disposition.

In the molten salt option, the fissile and/or fertile material is in solution with a salt, and kept in the liquid state during the entire life of the engine, see Fig. 3. In this case the requirements are:

- Optimized molten-salt composition compatible with LIFE specifications
- Controlled molten salt behavior in a drastic varying chemistry with time
- Corrosion-resistant fuel containment for the molten salt
- Pu solubility (not an issue in the Thorium fuel option)
- On-line cleaning process and chemistry (gas sparging and precipitation extraction due to FP formation)
- Production of a suitable wasteform for disposition

Very little will be discussed in this paper on the molten salt fuel option since a separate document covers the subject in detail [Moir et al. 2008].

Whatever the final fuel option will be, the dramatic change in fuel chemistry as a function of burn-up has never been explored in the past, and therefore adds challenges to the design of a fuel form that must retain its performance, and in particular its thermal and mechanical integrity,

during the entire life of the engine. In Fig. 4, we show as an example the amount of fission products and gases generated from DU fuel as a function of burn-up (% FIMA) [Shaw et al. 2008]. In the following, depending on the fuel option, the interaction of some of these elements with the fuel form will need to be carefully studied.

After a brief background, the solid fuel options will be examined in the context of thermal stability and integrity, and for each, a path forward with suggestions for specific research directions will be given. Since the molten salt option presents a suite of specific challenges that have been briefly discussed above, it was decided that a separate report would be dedicated to it.

Chapter B. Approaches to Solid Ultra-high Burn-up Fuel

The implementation of fuel cycles where high FIMA >50% is achieved coupled with a minimum number of fuel reprocessing/recycles are being proposed as a realizable objective for emerging critical reactor technology. While the accumulation of FP makes >90% FIMA of a uranium fuel form impossible (for fissile material such as ^{239}Pu this is possible), the need for very high burn-up is still economically desirable.

An interesting idea for a very deep-burn fuel cycle, whose proponents suggest could be “implemented in the near term”, is the Deep Burn-Modular High-temperature Reactor (DB-MHR) [Venneri 2005]. This reactor, which utilizes TRISO fuel, boasts a number of enhanced operational and performance features:

- Fuel containment to complete burn-up
- Repository containment
- He gas coolant transparent to neutrons
- Thermal spectrum and low damage to materials.

The DB-MHR is conceived as having applications to burning both Pu and MA as well as to play a role as a reactor for future sustained nuclear power growth. In this concept, a LEU fuel accounts for 4/5th of the core while a Pu+MA fuel accounts for the other 1/5th. By re-fabrication of the TRISO fuel and its re-use in the reactor, high burn-up can be achieved. While the outlook for high burn-up and ultra-high burn-up with TRISO fuel form appears to be optimistic based on early experimental work, considerable research will be required to achieve the reliability and economy (minimum number of recycles) necessary for this fuel form. We will discuss these research needs below.

The ability of a fuel form to achieve high- or ultra-high burn-up depends on several interacting variables. Simply stated, it is the changes in the fuel associated with neutron irradiation (fission and the resulting FP, displacement of atoms, nuclear transmutations, *etc.*), coupled with temperature and chemical and mechanical stresses that accumulate during the life of the fuel that can ultimately lead to failure of the nuclear material containment system.

Usually the nuclear component of the fuel at BOI consists of the fertile and fissile materials (isotopes of uranium) and possibly recycled Pu+MA. It is assumed that this nuclear material has been processed into a suitable form, a metal, or a ceramic (oxide, nitride, or carbide), a cermet, for example, of U-ceramic and a suitable metal. Usually, these nuclear fuel materials are compressed and sintered into pellets that are packed into hollow tubes (commonly made of zircalloy) that are then filled with a thermally conductive fluid and sealed, thus forming the fuel rod. Currently, researchers are studying even more complex fuel forms with the goal of achieving even higher burn-up.

Tristructural-isotropic (TRISO) Fuels

An interesting concept is the TRISO fuel that is a type of micro particle system consisting of a nuclear-fuel kernel surrounded in turn by multiple layers of low density and structural cladding. The fuel kernel may be composed of UO_2 , UC, or UCO as well as Pu or Pu+MA ceramics, and is coated with four layers of three isotropic materials. As shown in Fig. 5, the four layers are a porous buffer layer made of carbon, followed by a dense IPyC, followed by a ceramic layer of SiC to retain fission products at elevated temperatures and to give the TRISO particle more structural integrity, followed by a dense OPyC. TRISO fuel particles are designed not to crack due to the stresses from processes (such as differential thermal expansion or fission gas pressure) at temperatures beyond 1600°C , and therefore can contain the fuel in the worst imaginable accident scenario in a properly designed reactor. Two such reactor designs are PBMR, in which thousands of TRISO fuel particles are dispersed into graphite pebbles, and a prismatic-block gas cooled reactor (such as the GT-MHR), in which the TRISO fuel particles are fabricated into cylindrical compacts and placed in a graphite block matrix. Both of these reactor designs are HTGR, which is a type of VHTR, one of the six classes of reactor designs in the Gen-IV initiative.

TRISO fuel particles were originally developed in Germany for HTGR. The first nuclear reactor to use TRISO fuels was the AVR and the first power plant was the THTR-300. Currently, TRISO fuel compacts are being used in experimental reactors, the HTR-10 in China, the HTTR in Japan, and a facility to be developed starting in 2009 in South Africa. Table I summarizes TRISO fabrication and development that are currently in progress around the world, and undoubtedly a fair amount of knowledge has been gained on the TRISO option, as illustrated by the substantial quantities of coated particles, in excess of 60,000 kg, that have already been fabricated in facilities around the world, cf. Table II. Table III presents typical characteristics of TRISO-kernels and coatings in current applications in commercial reactors, DB-MHR and Russian WGPu disposition facilities. Figure 6 is an illustration of the TRISO fuel anticipated for use in this class of reactors.

Shortcomings of TRISO Fuel and Research Directions

TRISO fuels have been studied seriously since the 1950s first by the late Rudolf Schulten who conceived of encapsulating UO_2 or UC in a high temperature material (SiC) to achieve an intrinsically safe reactor. These fuels have been used as the basis for PBRs that today are being developed as modular systems of three, four, or eight reactors in a single plant. The integrated and synergistic nature of the TRISO particles is quite extraordinary as illustrated in Fig. 5 [Venneri, 2005; Hanson et al. 2001]. It can be seen that the materials actually work together to result in a containment system that is more than the sum of the individual parts. The performance of the particle essentially depends on the integrity of the SiC layer that acts as a diffusion barrier to metallic FP and as a pressure vessel of the particle.

TRISO fuel has the feature of offering a number of options for the implementation of its use in nuclear energy generation. First, the TRISO particle dimensions can be optimized to achieve the performance level required for high- and ultra-high burn-up. Fig. 7 illustrates three TRISO assemblies, each of which is optimal for a particular application. All three of the TRISO fuel types in TABLE III require important research activities related to their individual components and to how the components interact with each other at BOI and during and after irradiation.

The uranium fuel requires proof testing to assure processing methods resulting in predictable yield and reliability. Severe differences exist between TRISO particles produced in the USA and those produced in Europe, and more importantly, TRISO particles produced in the same batch often exhibit extreme differences in performance and failure rates. For the Pu and Pu+MA fuels standardized methods for production must be developed leading to predictable performance and reliability at high burn-ups approaching or exceeding 90% FIMA. Materials changes from the standard SiC coating and optimization of the low-density buffer layer are required. Of very high importance are the post-irradiation handling and properties of TRISO fuels. Development of particle recycling including composite disassembly should be pursued. High burn-ups imply and enable minimal reprocessing. However, to achieve maximum benefits we must be able to predict TRISO particle behavior and performance during cool-down and in the geological repository. Finally, and critical for licensing, we must develop a fundamental understanding of coating property data and associated integrated models including all failure mechanisms that can be included in the reactor materials database.

The TRISO capsule is the first barrier to FP release and is the key to the operational safety and licensing of reactors utilizing this fuel form. To date, two implementations of the TRISO particles have been studied: one is the pebble composite structure used in the PBMR (see Fig. 5), and the other is the prismatic carbon assembly block shown in Fig. 7, fueled with TRISO-composite cylindrical pellets as a part of the design of the General Atomics DB-MHR.

The TRISO particle is an extraordinary system of materials that, working together, result in performance exceeding the performance of the individual materials. An illustration of these forces is shown in Fig. 8. These forces are a consequence of radiation, temperature and time. Accurate structural analysis of the TRISO fuel at all stages of its use is a key to the development of ultra-high burn-up with this fuel form. PISA utilizing simple visco-elastic models can provide accurate predictions for materials performance providing that the dimensional and force data input to these models is suitably precise and known as function of the evolving chemistry.

Indeed, the chemistry of the fuel kernel as a function of burn-up and temperature is key. This includes liberation of oxygen and equilibrium pressures with FP, the forms of FP oxides, the equilibrium O₂ and CO pressure, the material phases, the oxygen getters, and the FP oxidation states. All of this leads to kernel swelling from the increase in the number of atoms and from void growth. FP release from the kernel builds gas pressure in the free volume. Understanding all these variables will lead to selection of the best form for the kernel composition;

UO₂/UC₂(UCO), PuO₂/Pu₂O₃ and with Np, Am, Cm, as well as a consideration of inert matrix fuels such as stabilized ZrO₂, with Pu, Am, and Cm.

The three TRISO layers, the IPyC, the SiC (or ZrC) and the OPyC are in constructive opposition to one another, the PyC is in tension whereas the SiC is in compression. This system is capable of holding pressures in excess of 150 MPa at temperatures up to 1600 °C. However, these three components face numerous materials issues over the course of a deep burn. These include:

- Behavior under irradiation *versus* initial structure
- Structural parameters affecting performance
- Optimum constitutive equations and thermo-mechanical properties
- Dimensional change (swelling) and creep under stress
- Phenomena leading to failure
- Mechanisms for fission product transport
- Decomposition under elevated temperature
- Reactions with fission products and CO

A detailed comparison of the differences between US manufactured and German manufactured TRISO fuels has recently been reported [Petti et al. 2003]. To date, the high-temperature and burn-up performances of the German fuels are substantially better than for the US fuels. Nevertheless, with regards to ultra-high burn-up, there are still numerous, and well understood, weaknesses associated with the SiC-based TRISO particle. It is useful to enumerate these problems, which recently have been outlined in some detail [Petti et al. 2003; Maki et al. 2007; Lauf et al. 1984; Diecker 2005], along with some directions in materials research that should lead to important fundamental understanding, and eventually mitigation or elimination of these shortcomings. As an example, Fig. 9 shows the replacement or the addition of ZrC as a way of improving the deep burn-up performance of TRISO fuel.

So far, the challenges associated with high-burn-up and high-temperature applications of TRISO-coated particle in VHTR and HTGR have been identified, and work is currently done to address them. Among them, it is worth mentioning the thermo-mechanical response of PyC, the FG pressure, the CO pressure, the kernel migration, the palladium attack, and the cesium release [Maki et al. 2007].

Thermo-mechanical response of PyC

The response (shrinkage or swelling) of PyC to neutron irradiation is very complex and not fully understood. While highly anisotropic, it depends on the irradiation temperature and the isotropy of PyC. With increasing temperature the shrinkage increases, as does the stress, however, this is offset by irradiation-induced creep that also depends on temperature and density of the PyC. At higher temperature, creep reduces stress in the IPyC layer. For the highly non-linear thermo-mechanical response of the coating system, creep dominates and the stress in the IPyC layer decreases as the irradiation temperature increases.

The structure-property relationships for irradiated PyC should be studied in detail to create accurate models for the materials property evolution from BOI to end of life.

Fission gas pressure

FG is produced during irradiation of the kernel of a coated particle. The resulting FG pressure depends on temperature, burn-up, diffusion properties, and time. Balancing kernel size against the available headspace provided by the low-density carbon layer is only a partial answer to the issues surrounding the presence of FG. Reduced kernel size leads to lower FG pressure, however, it also results in a faster migration of FP towards the SiC layer with subsequent issues of chemical attack.

Research aimed at designing a kernel system with a high degree of hold-up of FP would greatly enhance TRISO performance and increase the possibility for ultra-high burn-up.

CO pressure

CO is a direct consequence of the excess oxygen that results from UO_2 fuel and the inability for the resulting fission fragments to bind all the excess oxygen produced. This excess oxygen reacts with the buffer to form CO gas. Under the appropriate conditions of temperature and burn-up the CO contribution to internal pressure can exceed the contribution to the total pressure of the FG by as much as four times.

The role of the kernel chemistry is very important in controlling CO. Although good results have been obtained with UCO fuel more detailed work is required to understand all the properties of alternate kernel fuels. Another area of research is the use of non-fissile oxygen getters such as ZrC coatings around the kernel. The study of the evolution and performance of these advanced materials systems at high burn-up is needed.

Kernel migration

Kernel migration or the amoeba effect, illustrated in Fig. 10, is well known but inadequately understood. It appears as a tendency for the kernel to migrate up the temperature gradient [Maki et al. 2007]. In reality the effect is the consequence of carbon migration from the hot side of the kernel to the cool side. The phenomenon is observed in carbide fuel but it is particularly severe in oxide fuels. The phenomenon increases with time, temperature, thermal gradient, and CO production. In oxide fuels the excess oxygen forms CO by reacting with PyC. Understanding the details of the diffusion-chemical reaction is important since direct contact of the kernel with the SiC leads to rapid failure of the TRISO pressure vessel.

Kernel migration is a chemistry/diffusion phenomenon which although understood in a descriptive sense requires extensive research to fully comprehend the atomistic processes

involved. Both theoretical and chemical studies are warranted if reactor design and operations cannot be guaranteed to eliminate temperature gradients in the fuel, a likely situation.

Pd attack

Pd attack occurs in the SiC layer. This failure mechanism is preceeded and then facilitated by cracks in the IPyC layer [Lauf et al. 1984; Diecker 2005]. This is an example of a failure mechanism that must be understood in a synergistic manner to provide adequate predictions for the course of Pd penetration during deep burn of TRISO fuels. It has been observed that Pd quickly diffuses through the buffer and IPyC layers and then forms small nodules at the interface to the SiC layer [Maki et al. 2007]. The mechanism of “corrosion” of the SiC layer by FP Pd, schematically represented in Fig. 11, involves several steps, notably: (1) the production of Pd by fission in the fuel kernel, (2) the release of Pd from the fuel kernel, (3) the transport of Pd to the SiC layer through the IPyC layer, and (4) the reaction of Pd with the SiC layer, and experiments indicate that the slowest step that limits the Pd-SiC reaction rate is step (2) [Minato et al. 1990]. An important point that determines the availability of Pd is the fraction of the fissions that come from Pu. Hence, it has been observed that LEU fuels produce more Pd than HEU fuels. The penetration rate of Pd in the SiC layer has an Arrhenius-temperature dependence, as shown in Fig. 12, and the Pd-penetration rate is temperature dependent [Maki et al. 2007]. Even at the lowest temperature of a 1000 °C, 10 μm of reaction attack with the SiC layer would be observed in 3.2 years. Although the Pd attack was detected on both the hot and cold sides of the particle, the corroded areas and the Pd accumulation were distributed more prominently on the cold side of the particle. However the Pd attack may be more complex since it seems to depend on the details of the SiC-layer microstructure [Lauf et al. 1984]. It is also worth noting that the substitution of SiC by ZrC does not prevent the attack, and the formation of intermetallics such Pd₂Si and ZrPd₃ has been observed, however with a slower corrosion rate in the case of the ZrC layer than the SiC one [Ogawa et al. 1986]. Other elements such as Rh and Ru have also been shown to react with the SiC layer at rates that may affect fuel performance as well.

Research focused on holding-up the Pd in the fuel kernel could help make dramatic improvements in the performance of the high burn-up LEU or even NatU TRISO fuels. Additionally, the performance of other types of ceramic coatings such as ZrC may result in reducing the effects of Pd penetration. Stability studies of C-Si-X and C-Zr-X, where X=Pd, Rh, Ru would allow a proper evaluation of the thermodynamic force in phase formation. This knowledge coupled with kinetic studies of phase precipitation and evolution in the SiC or ZrC layer would allow a quantitative prediction of SiC attack as a function of time and burn-up.

Cesium release

It is important to study the high-temperature accident response of TRISO-coated particle fuels, particularly at high burn-ups. Some experiments have shown release of Cs but the reasons for the increased release are not known with certainty [Petti et al. 2003]. A photomicrograph of the SiC in a coated particle from one such test [Petti et al. 2003] is shown in Fig. 13. The SiC layer from

these particles does show some degradation. Two hypotheses can be formulated concerning the degradation: (a) Cesium attack of the SiC. (b) CO attack of the SiC layer [Petti et al. 2003]. However, there are not enough data to confirm or refute either of these two hypotheses [Petti et al. 2003].

The ultimate failure of a TRISO particle is the release of the FP and the fuel. Ultra-high burn-up will reduce margins and increase uncertainties. A research effort focused on failure mechanisms of the ceramic coating (SiC, ZrC...) are not only important for normal operations to high burn-up, but are also the central issue in accident scenarios and subsequent fuel cooling, and eventual geological storage. Furthermore, materials modifications, such as the addition of SiC fibers to SiC (SiC-SiC), and the materials engineering of ultra-tough ceramics using soft interfaces, offer opportunities to enhance performance of TRISO fuels and achieve the goal of ultra-high burn-up.

Inert Matrix (IMF) and Dispersed Fuels

Another concept, originally developed to burn Pu+MA in LWRs, is the broad class of inert matrix fuels (IMF). This fuel form is fabricated by blending the nuclear fuel material (UO₂, UC, or UCO) with inert matrix (non-fuel) material such as spinel or yttria. IMFs are produced by blending the nuclear-fuel into the matrix in either a homogeneous (solid-solution) known as a micro-dispersion, or a heterogeneous blend with nuclear fuel particles >100 µm known as a macro-dispersion. The usual form for an IMF is that of a cylindrical pellet (see Fig. 14) that fits into a metal cladding such as a zircalloy, and the free volume of the cladding is filled with a thermally conductive fluid and sealed.

The focus has shifted away from IMF usage in an LWR environment. The call for fast and efficient Pu-destruction in the existing fleet of LWRs is diminishing with new Fast Reactors being a future option. At the same time, the possible application area for IMF has widened. In new reactor types the inherent properties of IMF (*i.e.*, low thermal conductivity, high proliferation resistance, and softer mechanical properties) may be of importance. The research to date has indicated that the best possibilities lie with a yttria- or a ceria-stabilized matrix. This matrix material appears to exhibit irradiation behavior and FP containment that is satisfactory enough to be considered as a fuel form for high- and ultra-high burn-up. However, utilizing this technology at high temperatures ~1000 °C will require that instead of metal cladding one will have to consider either a ceramic- or a carbon-clad material similar to that being employed in pebble-bed modular or prismatic carbon HT-GCR. The IMF research results to date form, therefore, a valuable input for future nuclear fuel development [Hellwig et al. 2006].

The ceramic-based matrices (spinel, YSZ, MgO, *etc.*) are so far the best option. However these IMF have been proposed mostly for high-temperature applications (well above 1000 °C), *i.e.*, way beyond what the LIFE engine requires. Most ceramic-based IMF suffer from several drawbacks, namely: (1) Low thermal conductivity, (2) damage by fission fragments resulting in swelling and cracking under irradiation, and (3) process manufacturing of pellets with ceramic matrix and PuO₂ is complex and involves dust-forming operations. On the other

end metallic matrices do not suffer from these problems, and extrusion of fuel was used to prepare fuel pellets and pins. Among potential candidate, it is worth mentioning, Al, Zr, and ⁹⁵Mo. However these metallic matrices allow for very limited swelling and the process fabrication involves dust-forming operations.

Shortcomings of IMF and Research Directions

Starting in 1994 the study of IMF as a fuel form for the transmutation of Pu and MA in thermal reactors and advanced systems has increased. Motivated by the idea that energy production remains the most desirable disposition for Pu+MA, and to solve the problem of Pu surplus in the short and medium term it was suggested to burn, as quickly and completely as possible, excess Pu in existing LWR and HWR [National Academy of Sciences 1994]. The basic strategy was to apply a once-through IMF irradiation prior to geological disposal [Degueldre et al. 1996]. With the recent changes in nuclear energy strategy resulting in Fast Reactors being a future option, this motivation has lost momentum. “At the same time, the possible application area for IMF has widened: In new reactor types, the low thermal conductivity may be better acceptable, and the high-proliferation resistance and the softer mechanical properties may be of importance. Today’s IMF research results form therefore a valuable input for future nuclear fuel development [Hellwig et al. 2006], especially in the context of Gen-IV [Degueldre et al. 1999, 2001, 2006, 2003; US DOE Nuclear Energy Advisory Committee et al. 2002].

The idea of incorporating the fissile and fertile nuclear reactor fuel with a non-burnable material opens the door for truly inventing a broad spectrum of new technologically relevant material systems. Parameters that can be optimized in such a fuel form are:

- Operations at high temperatures
- Minimization of expansion due to radiation effects (so called soft mechanical properties)
- Retention of FP
- Optimization of heat capacity and thermal conductivity
- Post-irradiation retention properties

However, today only a small part of this materials design space has been explored. YSZ has proven to be a promising material to be the inert matrix for fuels. Macro- and micro-dispersions have been synthesized and tested in various reactors in the form of metal clad pellets, see Figs. 14 and 15.

However, the low thermal conductivity of YSZ is a severe limitation. To overcome this shortcoming, dual phase magnesia–zirconia ceramics doped with plutonia were studied as an IMF [Medvedev 2006]. The idea is that the MgO phase acts as an efficient heat conductor to increase thermal conductivity of the composite. Encouraging results have been obtained indicating that the MgO phase is left in tact and will provide the hoped for additional thermal conductivity.

Among the tools needed to advance the development of IMF is the capability to accurately model the thermodynamic properties of these complex materials, the properties of which rely on the beneficial precipitation of specific phases. Recently Arima and coworkers have applied equilibrium molecular dynamics with an ionic model to deduce the thermal conductivity of IMF zirconia fuels [Arima et al. 2006]. Their results are very encouraging and suggest that modeling capabilities in this area can be very valuable.

A more ambitious approach to modeling the thermodynamic properties that can be applied for predicting the thermal properties of other forms of nuclear fuels and materials for which the data are still unavailable or incomplete has been investigated by Sobolev and Lemehov [Sobolev et al. 2006]. Using a simplified model of the phonon spectrum, statistical thermodynamics, and the generalized Klemens model for thermal conductivity, the authors report obtaining useful relationships bounding the specific heat capacity, the thermal expansion coefficient, the bulk modulus and the thermal conductivity of dioxides, often used as components in IMF, were deduced in a quasi-harmonic approximation.

A research approach that combines the advantages of IMF with TRISO fuel forms may possibly lead to the ultra-high burn-up fuel forms needed to dramatically change the fuel cycle landscape for future generations.

Chapter C. Where Are We Today in the Context of LIFE?

TRISO Fuel Option

TRISO fuels have a long history of development research. While problems and weaknesses exist in TRISO fuels they are for the most part well identified and the research required to mitigate or overcome these weaknesses, while challenging, is not unreasonable or impossible. Figure 16 illustrates the extent of TRISO performance while also indicating the objectives and parameters associated with high and ultra-high burn-up fuel forms.

The failure mechanisms associated with high-burn-up are often the result of a system failure, and hence can be approached from that point of view. As noted earlier, the development of pressure in the TRISO capsule depends not only on FIMA, but also on the production of CO and the diffusion of the volatile FP from the interior of the kernel out. Hence a systems approach is clearly warranted in approaching the materials and technical challenges associated with extending TRISO performance to high- and ultra-high burn-up. At the same time the applications that are targeted by current TRISO research conducted especially in the USA (NGNP), Germany (HTGR), Japan, South Africa, France, and China show that the performance limits are very different, notably for power density, burn-up, fast fluence, and to some extent temperature, as summarized in Table V and Fig. 17 [Maki et al.; Latkowski 2008].

Although the temperature at which TRISO will be exposed under LIFE conditions is low (less than 800 °C) compared with what it is designed for (above 1100 °C), during the life of the TRISO particle, the chemistry will be drastically changing, as discussed in the introduction, see Fig. 4. In particular, the amounts of Pu and FP such as Pd have to be considered very seriously. Indeed according to Fig. 18, the Pu composition peaks around 30-40% FIMA, whereas the composition of Pd, and for that matter of other transition metals such as Mo, Ru, and Zr, keeps rising up to 100% FIMA. Hence, it is imperative that a validated approach to Pd (and other metals) attack of the SiC layer is put in place to predict as a function of time and Pd (and other metals) composition the penetration depth and the loss of performance of the SiC layer.

It is also important that attention is paid, with the changing chemistry, to predicting the melting temperature, and the formation of phases with time in the kernel region of the TRISO particle. For this purpose, based on the CALPHAD approach described in Appendix A, a thermodynamic database is under development as discussed in Appendix B.

Specific Research Directions

Below we review specific directions of research that will advance our understanding of materials to achieve a fuel form for ultra-high burn-up. Most of what we suggest is centered around the TRISO fuel form, whose nearly five decades of research and successes makes it an excellent platform for further materials system development. However, we also recommend research in two general areas of IMF, first an IMF kernel for TRISO fuels, and second a fully ceramic IMF

fuel form. While we have parsed these research directions based on the components of the fuel form we intend to keep keenly in mind the systems nature of the materials challenges.

Kernel

There is a major dilemma associated with developing TRISO fuel for ultra-high burn-up, and that is the conflict between reduced kernel size to minimize EOL gas pressure from volatile FP, and the economics of maximizing to the extent possible the power density of the fission fuel.

As discussed earlier, fuel chemistry is very important when considering the transport of carbon that results in the so-called amoeba affect. Good results have been obtained using UC or UCO as the fuel form, although carbon transport is still an issue. Understanding the details of the carbon transport mechanisms in different chemistries is very important in accurate predictions of fuel EOL and in also understanding the component of gas pressure arising from the production of CO-CO₂.

One of the most obvious changes that the fuel kernel will undergo is the transmutation of the fuel into FP. For UO₂, UCO or UC, the final fuel form will be ~95 at.% FP plus the carbon and oxygen of the original ceramic fuel. Ways to meet the following technical objectives should be researched;

- 1) A fuel composition and microstructure that maximizes the hold-up of both volatile FPs and corrosive FPs (Pd, Ag, *etc.*) in the fuel kernel.
- 2) A fuel kernel microstructure that accommodates FP and minimizes fuel kernel swelling. This might include research on low-density fuels with built-in headspace.
- 3) A fuel kernel material design that provides adequate thermal conductivity to minimize center-line temperatures in the TRISO particles.
- 4) A model describing the thermo-physical evolution of the fuel kernel as the fissile and fertile materials are converted primarily to FP.
- 5) A kernel barrier to assist in controlling oxygen fugacity to the rest of the TRISO particle, and to act as a diffusive barrier for FP transport.
- 6) Development of an inert matrix kernel with high fertile material content and good thermal conductivity to mitigate the effects of ultra-high burn-up as outlined by items 1-5. Recent success achieved at the Bochvar Institute in utilizing WGPu in a stabilized zirconia appear to be a promising example of an engineered IMF with good thermal and radiation properties.

PyC buffer

The PyC buffer layer serves two purposes in the TRISO fuel. First, is that it provides headspace to accommodate the volume increase in the fuel kernel, and second, it stops fission fragments emitted from the surface of the fuel kernel, keeping them from reaching the IPyC. Among potential research directions, it worth mentioning:

- 1) Optimal design for density and head-space performance.

- 2) Research of other materials and microstructures, such as porous media, aerogels, zerogels, *etc.*

IPyC

The IPyC is a critical structural element in the containment strategy of the TRISO particle. Its behavior under irradiation balances the inward forces of the SiC, and together the two structures provide a robust pressure vessel whose properties are sufficient to very high neutron doses. However, failure in the IPyC leads to failure quickly in the SiC that results in unavoidable structural failure of the TRISO particle. Hence, the following issues need to be addressed:

- 3) Behavior under irradiation versus initial structure.
- 4) Structural parameters affecting performance.
- 5) Best constitutive equations and thermo-mechanical properties.
- 6) Dimensional change, creep under stress.
- 7) Phenomena leading to failure.
- 8) Mechanisms for fission product transport.
- 9) Decomposition under elevated temperature.
- 10) Reactions with fission products and CO.

Ceramic capsule (SiC ZrC...etc)

By far the most experience with the ceramic shell of the TRISO particle has been obtained with SiC. Understanding the nature of all possible failure mechanisms for the ceramic shell is important if one hopes to successfully extend TRISO lifetime to beyond 90% FIMA and the use of fertile fuels with the concomitant increase in neutron fluence. Hence, all the issues related to the IPyC are also relevant for SiC and ZrC.

Japanese studies have reached the following positive indications for ZrC shells [General Atomics 2006]: (1) better performance against kernel migration failure and chemical attack by FP, including Pd; (2) better durability against pressure vessel failure at temperatures above 1600 °C (up to at least 2000 °C); and (3) better retention of FP, except Ru, particularly at temperatures of 1600 °C and above. However, as said before, in the context of the LIFE engine, the use of ZrC may not be adequate, since its purpose was originally to sustain high temperatures, which is not what LIFE specifications require.

TRISO systems issues

The failure mechanisms of TRISO fuel are well understood, and the research required to make improvements is well defined [General Atomics 2006]. Figure 19 illustrates the various failure mechanisms. Solutions to the problems mentioned above, and summarized in Fig. 20, should lead to improved manufacturing and materials modifications with, ultimately, V&V robustness and high burn-up that are desired for an advanced fuel capable of 90% FIMA and above.

Solid Hollow Core (SHC) Fuel Option

To accommodate the production of FG during burn-up, improve the resistance to thermal shock and fatigue, and improve fracture properties and toughness, the concept of a SHC fuel has been

considered. SHC fuel now refers, not to a particle (like in the case of TRISO), but to the pebble instead with dimensions as indicated in Fig. 21. This concept benefits to some extent from the knowledge gained so far on TRISO fuel particles, with a configuration that includes, at the center of the pebble, an expansion volume made of a porous carbon core, a sacrificial SiC, and a PyC transition layer. Beyond the volume occupied by the fuel itself, several layers act to maintain proper mechanical integrity of the pebble; they consist of a SiC sacrificial layer, a ZrC diffusion barrier, a PyC transition layer, and a high strength SiC/SiC fiber wrap in contact with a fiber-to-clad transition layer. The overall size of the pebble is between 2 and 4 cm. Among the issues that have to be addressed, it is worth mentioning:

- Fiber shrinkage and swelling that cause stress-induced debonding of the fiber/matrix interface, as also observed in the case of TRISO particle.
- Differential materials response under thermo-mechanical load.
- Irradiation swelling of the fiber, fiber/matrix interface (fiber coating), and the matrix.
- Factors that limit the range of operation, such as the decrease in thermal conductivity of the SiC/SiC composite layer with temperature and irradiation.
- Optimal volume occupied by the fuel, and overall thermal conductivity.
- Joining and fabrication anticipated prohibitive cost.

Specific Research Directions

As in the case of TRISO, FP attack to surrounding layered structures has to be thoroughly quantified, and suggestions for remedies will be required.

Inert Matrix Fuel (IMF) Option

To improve fuel performance for PWR and BWR several approaches have been considered that focus on increase in fuel content, lower temperature in the fuel element, extension of burn-up, and serviceability of the fuel elements operating under transient conditions. One of the promising approaches is the impregnation by a molten alloy in the inner space of a fuel element consisting of fuel granules arranged inside it.

Like for any other IMF, the concept itself is sound. Indeed, having a matrix that takes very little volume compared with the fuel itself, and can accommodate with its porous structure FG during burn-up with minimum swelling is appealing. The requirement is that the matrix should be irradiation resistant so that it keeps its thermal and mechanical integrity during the entire life of the fuel particle.

In addition and in comparison with the oxide version of IMF, metallic IMF offer high effective fuel density and high thermal conductivity, efficient metallurgical bond between the fuel and the cladding, protection against fuel-cladding interaction, and uniform distribution of fuel particles in the metallic matrix. Elements of comparison between conventional fuel element designs are shown in Table VI [Savchenko et al. 2007a, 2008a].

A new class of metallic IMF has been recently developed at the A.A. Bochvar All-Russia Institute of Inorganic Materials (VNIINM) in Moscow (Russia) that involves an environment-

friendly and simple fabrication process, leads to high fuel density, low fuel temperature (600-700 °C), workability in transients, high resistance to irradiation and corrosion, high burn-up (100 MW.d/kg-U in thermal reactors and up to 200 MW.d/kg-U in fast reactors), and solution to the closing of the fuel cycle [Savchenko et al. 2006a, 2006b, 2007a, 2007b, 2008a, 2008b, 2008c, Savchenko and Konovalov 2008]. To improve the properties of metallic IMF, low-melting point Zr brazing alloys have been developed. Since Zr itself is a relatively high-melting point metal (1855 °C), the original idea was to alloy Zr in a way that the melting point was below 825 °C since most actinide-based fuels stay stable in their solid form below 950 °C. Several classes of novel Zr-based brazing alloys have been developed as indicated in Table VII. All of them display deep ternary or quaternary eutectics with low-melting temperature, *i.e.*, from 690 to 860 °C.

Several versions of IMF were proposed:

- (1) Isolated arrangement of fuel that involves an Al or Zr-based matrix and PuO₂ or MA powder that is an acceptable proposal for thermal and fast reactors, cf. Fig. 22. The advantages of such version are: minimum dust-forming operations with Pu, three-barrier protection against corrosion, adaptation for minimizing swelling, and finally relatively cold fuel.
- (2) Heterogeneous arrangement of fuel, that was primarily designed for thermal reactors, with as a fuel PuO₂ or (Er,Y,Pu,Zr)O₂ and a matrix made of Al or Zr-based alloy, cf. Fig. 23. In this case, the advantages are: usage of an impregnation technology, accommodation for minimizing swelling, and cold fuel.
- (3) Fuel within a Zr-based frame with a two-stage fabrication that consists of a Zr frame produced by a capillary-image method, and PuO₂ or MA introduced into the frame pores, cf. Fig. 24 [Savchenko et al. 2008c].

Consider for example, that the initial components of the combined fuel are granules of DU alloys, PuO₂ powder, and granules of Zr-alloy matrix. The characteristics of the novel fuel and the fuel composition are tabulated in Tables VIII and IX together with the appearance of the original components shown in Fig. 25. These alloys exhibit at 500 °C excellent compression strength of about 500 MPa, and thermal conductivity in the range of 20 to 30 Wm⁻¹K⁻¹, with a fuel content around 11.0 g.cm⁻³.

An example of fabrication of fuel-element with such a capillary-impregnation method is summarized in Figs. 26 and 27.

By adjusting the size ratio of fuel over matrix granules, one can achieve high-fuel content, with, volumes between 50 and 60% for the fuel form, 7 and 15% for the matrix, and 30 and 40% for the pores (without PuO₂). Hence, the high-fuel content (U and Pu), compared with, *e.g.*, MOX fuel, leads to a high conversion ratio, and consequently maximum heat transfer, and because of the low damage of the fuel by FP a low swelling compared with the U-Pu-Zr fuel. Furthermore,

metallic dispersion fuel elements guarantee high thermal conductivity, efficient metallic bond between the fuel and the cladding, and a decrease in the fuel temperature. It is also worth noting that the added solute elements to Zr not only decrease the melting temperature of the alloy, but also promote a natural beneficial coating of the cladding against FP attack. This coating acts as a diffusion barrier against fuel element (U, Pu, and MA), and FP attack of the cladding materials.

Some of these formulations have been studied in in-pile tests, cf., *e.g.*, Table X, under accident conditions, and in transient conditions of repeated thermal cycles and shocks [Savchenko et al. 2006b, 2008b]. So far the response of these IMF under these stringent conditions has been promising (*e.g.*, no swelling, excellent resistance to FP and FG “attacks”, mechanical integrity of the cladding, excellent thermal transport) although outside LIFE conditions.

Specific Research Directions

Regarding the issue of phase formation and transformations in metallic IMF, several questions need to be addressed:

- Optimal metallic inert-matrix materials selection under LIFE conditions, with optimum neutron spectrum.
- Suitable metal-matrix composition that can sustain ultra-high burn-up.
- Thermal behavior of the metallic matrix as a function of burn-up in a varying chemistry.
- Effect of FG on IMF performance.
- Interaction of the metallic matrix, in the presence of FP, with cladding.
- Optimal size ratio of fuel over metal granules.

Once these questions are satisfactorily answered, it is apparent that metallic IMF with their cladding could be considered as a fully viable option for pebbles for the LIFE engine.

A research approach that combines the advantages of IMF with TRISO fuel forms may possibly lead to the ultra-high burn-up fuel forms that satisfy LIFE requirements.

Conclusions

Based on the output of a recent solid-fuel working group presentation [Brown et al. 2008], the viability of each of the three options, *i.e.*, TRISO fuel, SHC fuel, and IMF that were discussed in this report, depends on the mission of the LIFE engine that is, either WGPu disposition, DU/NatU or SNF burning. A summary of this output is shown in Table XI.

For Pu disposition, because the dpa limit imposed on graphite is not so severe, the disposition of WGPu could be taken care of with a TRISO-like configuration. For the other two missions that require ultra-high burn-up, the viability of a TRISO option is remote since graphite would need to be replaced so that the swelling at dpa greater than 10 does not become a problem. SHC fuel could become an acceptable option for the last two missions, although the complexity of the fabrication by design and the problems that are not insurmountable and share some commonality with those associated with TRISO still need to be solved. The IMF option is a highly promising one, especially for the burning of DU/NatU and SNF, but as in the case of the SHC fuel option, a research and development plan is required before anyone of these two options can be certified.

Thus, it becomes apparent that the best approach to achieve the advancement of the burn-up capability of reactor fuels that meet the requirements of the LIFE engine is one that embraces both experiments and modeling. The combination of well-developed modeling and computer simulation capabilities gives reasons to expect significant contributions to the development of ultra-high burn-up fuels, and be able to tackle the issues that are presented in a summary form in Table XII.

Our goal is to validate advanced modeling methods that can then serve as the basis for designing integrated experiments to be performed in real situations. Incorporating High Performance Computational Materials Science into fuel modeling is a need unanimously recognized by the scientific community as a high pay off investment that will help advance the knowledge of these materials and the design of better materials for extreme environments.

In the three solid fuel options that have been discussed in this report, there is commonality in some of the main issues, as far as the main thrust of phase formation and transformation in transmutation fuels is concerned, cf. Table XI. Indeed, in all cases the dramatic change in chemistry as a function of time, or burn-up, raises the important question of phase formation and precipitation that will clearly impact volumetric change and swelling. In addition the production of FP and FG may have a detrimental effect on the containment matrix and the cladding of the particle or the pebble. In the case of TRISO and SHC fuels, the attack by some of the FP has to be quantified as a function of time so optimal thickness of the functional layers is achieved. In the case of metallic IMF fuel, appropriate elements that form the containment matrix and optimal matrix composition have to be selected. Once a sound thermodynamic basis has been established, the impact of different microstructural elements (*e.g.*, concentrations of MA and FP) on thermal conductivity and mechanical degradation of the fuel, that are key predictors of fuel

performance, can be evaluated by appropriate methods. In the DOE complex and abroad (especially in France, Japan, and Russia) significant work is underway to study and develop material systems leading to significant advances in the area of nuclear fuels performance modeling through the introduction of new materials or material combinations.

Another relevant and equally important thermodynamic-problem that is ideally suited for a computational approach is the thermal migration or Soret effect, appearing in systems under thermal gradients such as the nuclear fuels in the LIFE engine, which in one of its manifestations is at the origin of the so-called amoeba effect, in nuclear fuels, either ceramics or metals. This non-equilibrium process is complex and irreversible, leading to failure of the fuel-cladding assembly. A combination of thermodynamic (for the evaluation of the energetic driving force) and kinetic (*i.e.*, species mobility and energy barriers for the evaluation of the temporal evolution of phases) data as input to coarse-grained methods based on the phase-field methodology (PFM) is the path forward to predicting the above mentioned effects in materials that are defined not only by their composition but also their microstructure. As a result, a robust understanding of the complex physical behavior of mixed actinide ceramics and metals has the potential for significant impact on advanced nuclear energy systems and the realization of the idea of a proliferation-resistant nuclear fuel scheme. The physical and chemical properties of such fuel materials must be determined and understood at a fundamental level if we are to accelerate their development. A combination of thermodynamic modeling and advanced theory, along with a robust experimental program, will significantly advance our understanding of mixed actinide metals. DTA and DSC studies supplemented by diffusion couple experiments are required to verify and validate the modeling that is performed on the statics and kinetics of phase formation and transformation in fuels. Furthermore, it is worth noting that TEM is the appropriate approach for characterizing the bonding-properties of complex systems by making use of focused electron beams. Indeed, TEM offers unsurpassed spatial resolution and determination of crystallographic orientation. In multi-phase-systems, the TEM's nano-scale analytical spot size can resolve each phase independently, a feature that should prove invaluable when studying complex mixed actinide compounds, and extract the bulk properties (*e.g.*, bulk modulus, Young's modulus, shear constants) that are useful to assess mechanical performance of nuclear fuels under normal and accidental conditions. The multi-physics issues that need to be addressed are summarized in the flow chart presented in Fig. 28 that shows the relations between research tools and topics, and properties and performance of solid nuclear fuels, with special emphasis on how thermodynamics and kinetics of phase formation and transformation in transmutation fuels are tied to properties and performance of advanced nuclear fuels.

The complexity of the technological problem calls for a strategy that addresses a combination of modeling and experiment focused on specific effects. In addition to utilizing published data, a series of targeted experiments should be carried out on model fuels and surrogate materials. The effects of FP damage, the presence of actinides, transmutants, and FP, should each be

individually addressed. For each case, the effectiveness of the sub-species (*i.e.*, the type of actinide or transmutant) on fuel stability should be determined.

While a thermodynamic-centric roadmap is extremely important for designing next-generation nuclear reactor fuels, so too are bulk physical properties, such as swelling, strength, ductility, and overall thermal and mechanical performance as functions of temperature, composition, and time as they affect operations and safety. Although these additional links will be explored in more details in other reports that are being put in place on materials for LIFE, a fundamental knowledge of the chemistry of nuclear fuels and its temporal evolution under specific external conditions is crucial for designing an optimum mission-dependent fuel for LIFE. In Part II of this report, some of the more urgent issues that have been identified here will be addressed with modeling tools already in place and some others that are currently under development.

Acknowledgments

The authors gratefully acknowledge input and comments from the LIFE materials team. PT and MJ gratefully acknowledge fruitful discussions with Claude Degueldre (Paul Scherrer Institute, Switzerland) and Alexey Savchenko (Bochvar Institute of Inorganic Materials, Russia) on dispersed matrix fuels. Work performed under the auspices of the U.S. Department of Energy by Lawrence Livermore National Laboratory under Contract DE-AC52-07NA27344.

Bibliography

T. Arima, S. Yamasaki, K. Yamahira, K. Idemitsu, Y. Inagaki, and C. Degueldre, “Evaluation of thermal conductivity of zirconia-based inert matrix fuel by molecular dynamics simulation”, *Journal of Nuclear Materials* **352**, 309–317 (2006).

N. W. Brown, T. Marcile, M. Caro, A. Caro, J. Mariam, P. E. A. Turchi, P. Demange, L. Zepeda-Ruiz, W. Halsey, H. Shaw, J. Blink, M. J. Fluss, and L. Kaufman, “LIFE solid fuel options”, internal LLNL presentation of the LIFE Solid Fuel Working Group (September 2008).

D.C. Crawford, D.L. Porter, and S.L. Hayes “Fuels for sodium-cooled fast reactors: US perspective”, *J. Nucl. Mater.* **371**, 202-231 (2007).

C. Degueldre, U. Kasemeyer, F. Botta, and G. Ledergerber, Plutonium incineration in LWRs by a once through cycle with a rock-like fuel, *Mater. Res. Soc. Proc.* **412**, 15 (1996).

C. Degueldre and J. M. Paratte. “Section 1: Introduction: Concepts for an inert matrix fuel, an overview”, *J. of Nucl. Mater.* **274**, 1-6 (1999).

C. Degueldre, M. Pouchon, M. Döbeli, K. Sickafus, K. Hojou, G. Ledergerber, and S. Abolhassani-Dadras, “Section 3: Fundamental radiation effects in inert matrix fuels and nuclear waste materials: Behavior of implanted xenon in yttria-stabilised zirconia as inert matrix of a nuclear fuel”, *J. of Nucl. Mater.* **289**, 115-121 (2001).

C. Degueldre and T. Yamashita, “Inert matrix fuel strategies in the nuclear fuel cycle: the status of the initiative efforts at the 8th Inert Matrix Fuel Workshop”, *J. of Nucl. Mater.* **319**, 1-5 (2003).

C. Degueldre, “IMF 10 Editorial note”, *J. of Nucl. Mater.* **352**, 254-255 (2006).

Jane T. Diecker, “Development of a Gas Cooled High Temperature Reactor TRISO-coated Particle Fuel Chemistry Model”, *Master of Science Thesis*, MIT (June 2005); and references therein.

S.A. Ershov, V.P. Kostomarov, and Y.I. Stelyuk, “Inert matrix fuel in dispersion type fuel elements”, *J. of Nucl. Mater.* **352**, 372-377 (2006).

Goverdhan Reddy Gajjala, “Interaction between Pd and SiC: A study for TRISO nuclear Fuel”, Master Science Degree in Engineering from the University of Nevada, Las Vegas (May 2006) and references therein.

General Atomics, “Coated Particle Fuel – Fuel manufacturing and performance for LLNL” (June 29, 2006).

D. L. Hanson and J. J. Saurwein, issued by General Atomics for the DOE “Development Plan for Advanced High Temperature Coated-Particle Fuels”, PC-000513.Rev (August 2001) 161 pages.

Ch. Hellwig, M. Streit, P. Blair, T. Tverberg, F.C. Klaassen, R.P.C. Schram, F. Vettraino, and T. Yamashita, *Journal of Nuclear Materials* **352**, 291-299 (2006).

J. Latkowski, private communication (August 2008).

R. J. Lauf, T. B. Lindemer, and R. L. Pearson, “Out-of-reactor studies of fission product-silicaon carbide interactions in HTGR fuel particles”, *J. of Nucl. Mater.* **120**, 6-30 (1984).

John T. Maki, David A. Petti, Darrell L. Knudson, Gregory K. Miller, “The challenges associated with high burnup, high temperature and accelerated irradiation for TRISO-coated particle fuel”, *J. of Nucl. Mater.* **371**, 270–280 (2007).

P.G. Medvedev, J.F. Jue, S.M. Frank, and M.K. Meyer, *Journal of Nuclear Materials* **352**, 318-323 (2006).

Kazuo Minato, Toru Ogawa, Satoru Kashimura, Kousaku Fukuda, Michio Shimizu, Yoshinobu Tayama, and Ishio Takahashi, “Fission product palladium-silicon carbide interaction in HTGR fuel particles”, *J. of Nucl. Mater.* **172**, 184-196 (1990).

V. Mishunin, S. Maranchak, Z. Petrova, and A. Kozlov, “Capillary impregnation technology for novel types of fuels”, *J. of Nucl. Mater.* (2007) doi:10.1016/j.jnucmat.2007.09.043.

R. W. Moir, H. Shaw, P. E. A. Turchi, L. Kaufman, and J. Latkowski, “Molten salt fuel option for Life”, LLNL Report (September 2008).

National Academy of Sciences (USA), Management and disposition of excess weapons plutonium. National Academy Press, Washington DC, USA (1994).

T. Ogawa and K. Ikawa, “Reactions of Pd with SiC and ZrC”, *High Temp. Sci.* **22**, 179-193 (1986).

D.A. Petti, J. Buongiorno, J.T. Maki, R.R. Hobbins, G.K. Miller, “Key differences in the fabrication, irradiation and high temperature accident testing of US and German TRISO-coated particle fuel, and their implications on fuel performance”, *Nucl. Eng. and Design* **222**, 281-297 (2003).

A.M. Savchenko, A.V. Vatulin, A.V. Morozov, I.V. Dobrikova, S.A. Ershov, S.V. Maranchak, Z.N. Petrova, and Y.V. Konovalov, “Inert matrix fuel with low melting point zirconium brazing alloys”, *J. of Nucl. Mater.* **352**, 334-340 (2006).

A.M. Savchenko, A.V. Vatulin, A.V. Morozov, V.L. Sirotin, I.V. Dobrikova, G.V. Kulakov,

S.A. Ershov, V.P. Kostomarov, and Y.I. Stelyuk, “Inert matrix fuel in dispersion type fuel elements”, J. of Nucl. Mater. **352**, 372-377 (2006).

A.M. Savchenko, I. Konovalov, A. Vatulin, A. Morozov, V. Orlov, O. Uferov, S. Ershov, A. Laushkin, G. Kulakov, S. Maranchak, and Z. Petrova, “Dispersion type zirconium matrix fuels fabricated by capillary impregnation method”, J. of Nucl. Mater. **362**, 356-363 (2007).

A.M. Savchenko, I. Konovalov, A. Vatulin, A. Morozov, O. Uferov, E. Glagovsky, S. Ershov, V. Mishunin, S. Maranchak, Z. Petrova, and A. Kozlov, “Capillary impregnation technology for novel types of fuels”, J. of Nucl. Mater. (2007) doi:10.1016/j.jnucmat.2007.09.043.

A.M. Savchenko, I.I. Konovalov, A.V. Vatulin, E.M. Glagovsky, and O.I. Uferov, “New Concept of Designing Pu and MA Containing Fuel for Fast Reactors” (preprint, July 2008).

A.M. Savchenko, I.I. Konovalov, and T. Totev, “MetMet fuel with zirconium matrix alloys” (preprint, July 2008).

A.M. Savchenko, A.V. Vatulin, E.M. Glagovsky, I.I. Konovalov, A.V. Morozov, S.A. Ershov, V.A. Mishunin, G.V. Kulakov, V.I. Sorokin, A.P. Simonov, Z.N. Petrova, and V.V. Fedotov, “Main results of the development of dispersion type IMF at A.A. Bochvar Institute” (preprint, July 2008).

A.M. Savchenko and I.I. Konovalov, “Dispersion type fuel element for VVER, RBMK, CANDU, and BN-800 reactors, to burn MA and as an alternative to MOX fuel rods” (preprint, July 2008).

H. Shaw and J. Latkowski, private communication (2008).

V. Sobolev and S. Lemehov, Journal of Nuclear Materials **352**, 300-308 (2006).

US DOE Nuclear Energy Advisory Committee and the Generation IV International Forum, GIG-002-00 “A Technology roadmap for Generation IV nuclear energy systems” (December 2002) 97 pages, <http://gif.inel.gov/roadmap/>.

F. Venneri, “Destruction of nuclear waste using MHR technology”, General Atomics presentation to LLNL (April 2005).

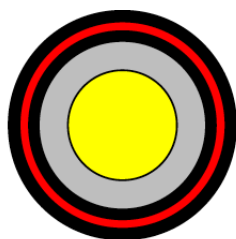
Tables

Reactor/ Manufacturing	Country	Fuel Description		U/Th Quantity (kg)
ROVER/GA & LANL	US	BISO	Extrusions	14,000
DRAGON	UK	BISO/TRISO	Compacts	1,000s
Peach Bottom I/GA	US	BISO	Compacts	3,500
UHTREX/GA & LANL	US	TRISO (Early)	Extrusions	200
Fort St. Vrain	US	TRISO	Compacts	33,400
AVR	Germany	BISO/TRISO	Spheres	2,200
THTR/Nukem	Germany	BISO	Spheres	7,700
CNPS/GA	US	TRISO	Compacts	94
HTTR/NFI	Japan	TRISO	Compacts	900
HTR-10	China	TRISO	Spheres	140
Russia, Belgium, France Korea, India, South Africa	various	BISO/TRISO	-----	Small

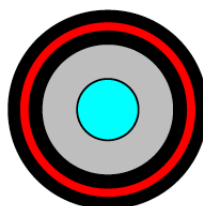
Table I. Partial view of the LIFE engine that shows where the molten salt blanket (in red) is located.

Coated Particle Fabrication Facility	Location	Fuel
NFI	Japan	TRISO-Coated UO_2 in annular compacts
INET	China	TRISO-Coated UO_2 in spherical fuel elements
ORNL	US	Various kernels TRISO-Coated in cylindrical compacts
BWXT	US	UO_2 and UCO kernels
CEA	France	Experimental Coated Particle Facilities
KFA Karlsruhe	Germany	Plutonium and actinide kernels
Bochvar Institute	Russia	TRISO-Coated Uranium & Plutonium
Pebble-Bed Project	South Africa	TRISO-Coated UO_2

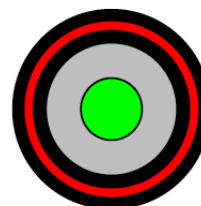
Table II. Substantial quantities of coated particles have already been fabricated in facilities throughout the world [Vennerri 2005].



Commercial LEU
GT-MHR (25% FIMA)



DB-MHR (70% FIMA)



Russian WGPu
(>70% FIMA)

Features	KERNEL Specifications					
	Commercial		DB-MHR		Russian WPu	
Composition						
Element/Atom %	20% enr U	100%	Pu	85	W Pu	100%
			Np	5		
			Am	10		
Diameter (_ m)	350		200		200	
Density (g/cm3)	>10.5		>10		>10.3	
Oxygen Management	UO ₂ , UC ₂ Mixture (UCO)		O/Pu<1.7, oxycarbide, O ₂ getters		O/Pu<1.7, oxycarbide, O ₂ getters	
TRISO Coating						
Coating Description	Coating Thickness (_ μm)					
Buffer Layer	100		>100		100	
IPyC	35					
SiC	35					
OPyC	40					

Table III. Kernel and TRISO coating specifications in some current applications [General Atomics 2006].

Inert Matrix type	Inert Matrix formula
Element	C, Mg, Al, Si, Cr, V, Zr, Mo, W
Intermetallics	AlSi, AlZr, ZrSi
Alloy	Stainless steel, Zr alloys
Carbide	¹¹ B ₄ C, SiC, TiC, ZrC
Nitride	AlN, TiN, ZrN, CeN
Binary oxide	MgO, Y ₂ O ₃ , ZrO ₂ , CeO ₂
Ternary oxide	MgAl ₂ O ₄ , Y ₃ Al ₅ O ₁₂ , ZrSiO ₄
Oxide solid solution	Y _y Zr _{1-y} O _{2-y/2} , Mg _(1-x) Al _(2+x) O _(4-x)

Table IV. Classes of inert matrices that have been proposed as candidates for IMF.

Comments	Burnup (% FIMA)	Temperature (°C)	Fast Fluence ($\times 10^{25}$ n/m ²)	Packing Fraction (%)	Power Density MW/m ³
USA (NGNP)	15-10	1250	4	<35	6
Germany (HTGR)	8	1100	3.5	10	3
Japan	4	1200	4	30	3-6
South Africa	8-10	1100	3.5	10	3
France	10-15	1100-1200	4	10-15	3-6
China	8	1100	3.5	10	3
LIFE	99	700-800	1800	~30	~100

Table V. Comparison of fuel service conditions [Maki et al. 2007, Latkowski 2008].

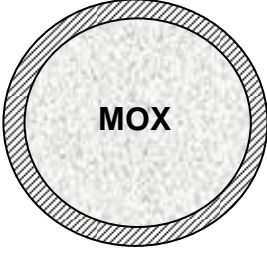
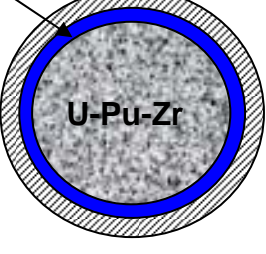
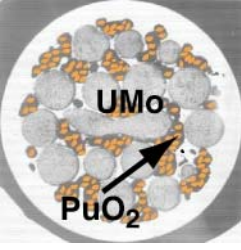
Parameters	MOX (U, Pu)O ₂ Fuel	U-20Pu-10Zr Alloy	Combined UMo-PuO ₂ Fuel
Fuel element design	Container	Container	Dispersion
Fuel element design			
Effective density of heavy actinides under fuel cladding, ρ^{eff} , g/cm ³	8.3-8.5	11.0	10.8-11.0
Content of fuel in fuel element (% of theoretical)	80-85	75	75 (55+20)
Maximal temperature of fuel, °C	2000-2250 (IFR,EFR)	<800 (IFR)	790 (BN-K)
Fuel (FP) – cladding interaction	Average interaction	High interaction	No interaction
Fuel – cladding gap	0.1 mm He	0.7 mm Na	0.0 mm Metallurgical bond
Thermal conductivity of fuel, W/m.deg	2-4	15-20	20-30
Adaptability of fuel element fabrication	Average	Average	High
Environmentally clean production	Low	Low	High

Table VI. Comparative design characteristics of container-type fuels (MOX and U-20Pu-10Zr metal fuel), and novel combined UMo-PuO₂ dispersion fuel for fast reactors [Savchenko et al. 2007a, Savchenko et al., 2008a, Crawford et al. 2007].

Group #	Alloy Composition (wt.%)						Melting T (°C)	Impregnation T (°C)
	Zr	Ti	Fe	Cu	Be	Nb		
1	Base	5-20	4-7	1-3	1.5-2.5	–	690-720	780-810
2	Base	–	4-8	0.5-3.0	2-3	1-3	780-810	850-870
3	Base	5-10	8-14	8-14	–	–	810-820	880-890
4	Base	–	6-12	6-12	–	–	850-860	900-910

Table VII. Alloy composition (in wt.%), melting and brazing temperatures (T) of potential Zr-based brazing alloys [Savchenko et al. 2006a].

	Components	Granules size, μm	Melting Temperature, °C
Metal fuel	U-(3-9)Mo U-(5-10)Zr U-(2-5)Zr,Nb U-(3-9)Mo-(0.1-0.6)C	500-1200	1200-1300
Zr-matrix alloy	Zr-(1.5-2.5)Be-(4-7)Fe Zr-(6-12)Fe-(6-12)Cu	100-300	800 860-900
PuO ₂	–	20-70	2200

Table VIII. Components, granule size, and melting temperature of the U-PuO₂ fuel [Savchenko et al. 2008a].

Fuel Components	Volume fraction, %	U(Pu) content under fuel cladding, g/cm ³	Melting Temperature after Manufacturing, °C
Metal fuel	55-60	9-10	1300-1400
Zr-matrix alloy	7-15	–	1150-1250
PuO ₂	10-20	0.9-1.8	2200
Pores	10-15 (30-40 without PuO ₂)	–	–

Table IX. Volume fraction, fuel content, and melting temperature after manufacturing of the combined U-PuO₂ fuel [Savchenko et al. 2007b, Savchenko et al. 2008a].

Fuel	Temperature clad/fuel, °C	Fuel element type	Burn-up	
			g-fuel/cm ³	MW.d/kg U
UO ₂ +Al alloy	350/370	VVER	0.8	100
UO ₂ +Zr alloy	300/500	Fuel composition	0.8	100
UO ₂ +Zr alloy	330/500	RBMK	0.4	55
UO ₂ +Zr alloy	330/440	VVER-440	0.45	60
UO ₂ +Zr alloy	600/750	Special	1.5	200

Table X. In-pile tests of prototype fuels with UO₂ [Savchenko et al. 2008c].

Mission	Solid Fuel Option		
	TRISO Fuel	SHC Fuel	IMF
WGPu Disposition	Good possibility with minimum development	Not needed for this application	Possibly not needed for this application
DU/NatU >97% burn-up	Not suitable because of graphite	Promising but requires R&D	High potential but requires R&D
SNF >97% burn-up	Not suitable because of graphite	Promising but requires R&D	High potential but requires R&D

Table XI. Summary of the output of the Solid Fuel Working Group on the *a priori* adequacy of the known options [Brown et al. 2008].

Problem	Low	Medium	High
Variable Chemistry			X
Radiation Swelling			X
FP Diffusion and Attack		X	
Abrasion and Corrosion Attack		X	
FG Pressure	X		
Thermal Pulsing	X		
Kernel Migration	X		

Table XII. Challenges facing all solid fuel options [Brown et al. 2008].

Figures

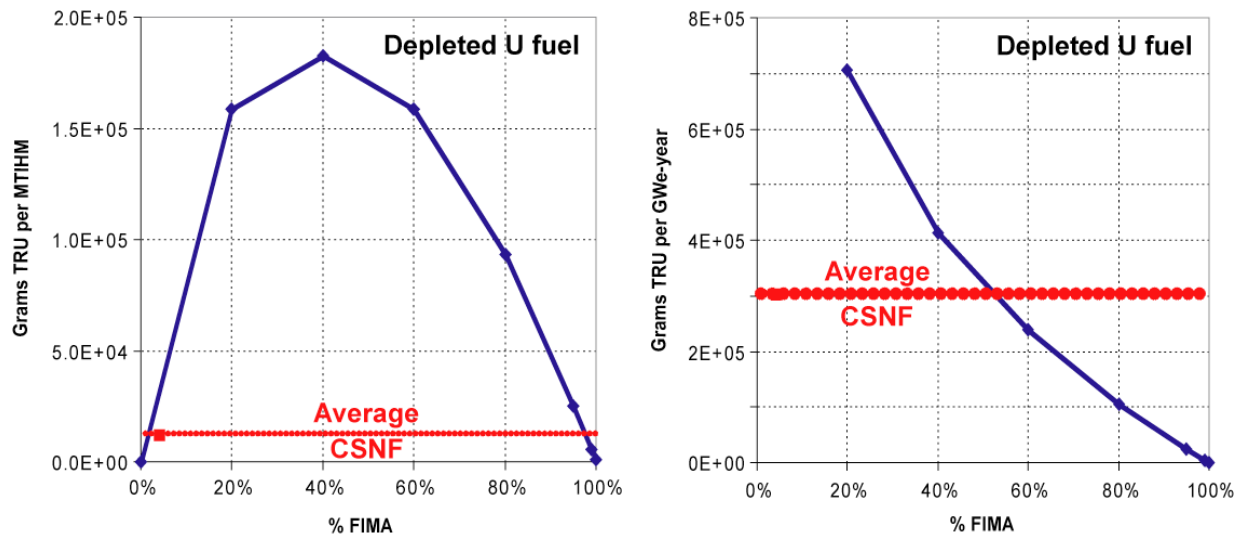


Figure 2. TRU formed as a function of FIMA, in grams per MTIHM (left) and per GWe-year (right) [Shaw and Latkowski 2008].

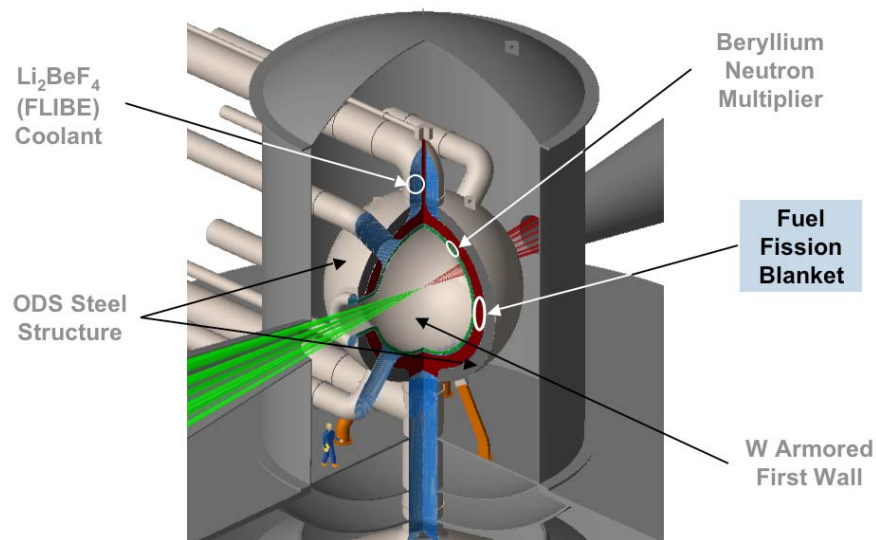


Figure 2. Partial view of the LIFE engine that shows (in red) where, in the solid fuel option, the fuel is located in the fuel fission blanket.

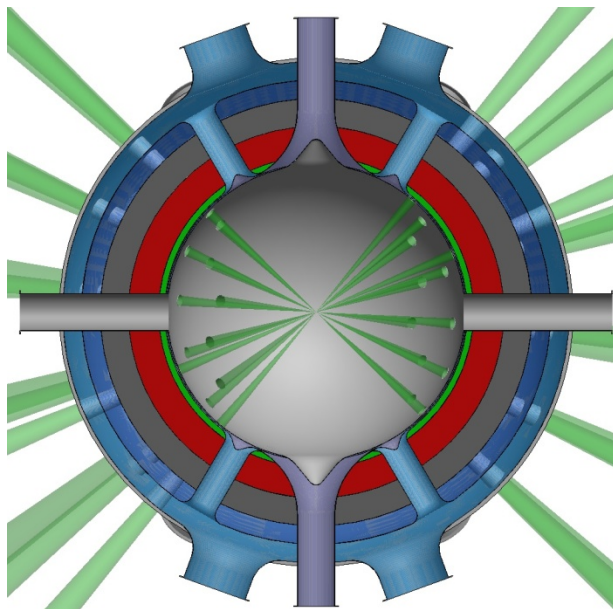


Figure 3. Partial view of the LIFE engine that shows where the molten salt blanket (in red) is located.

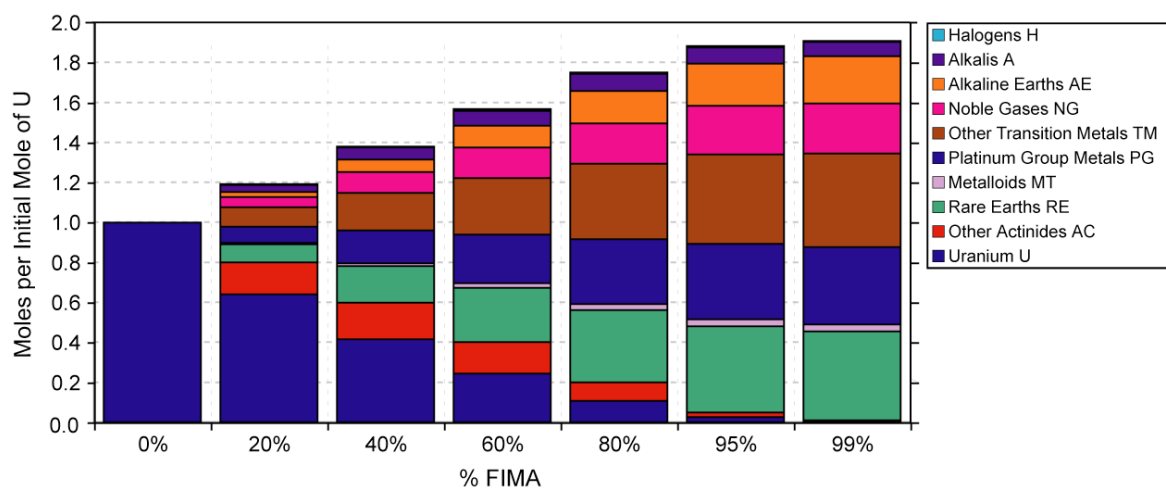


Figure 4. Fission products and gases generated by a DU fuel as a function of burn-up (% FIMA) [Shaw and Latkowski 2008].

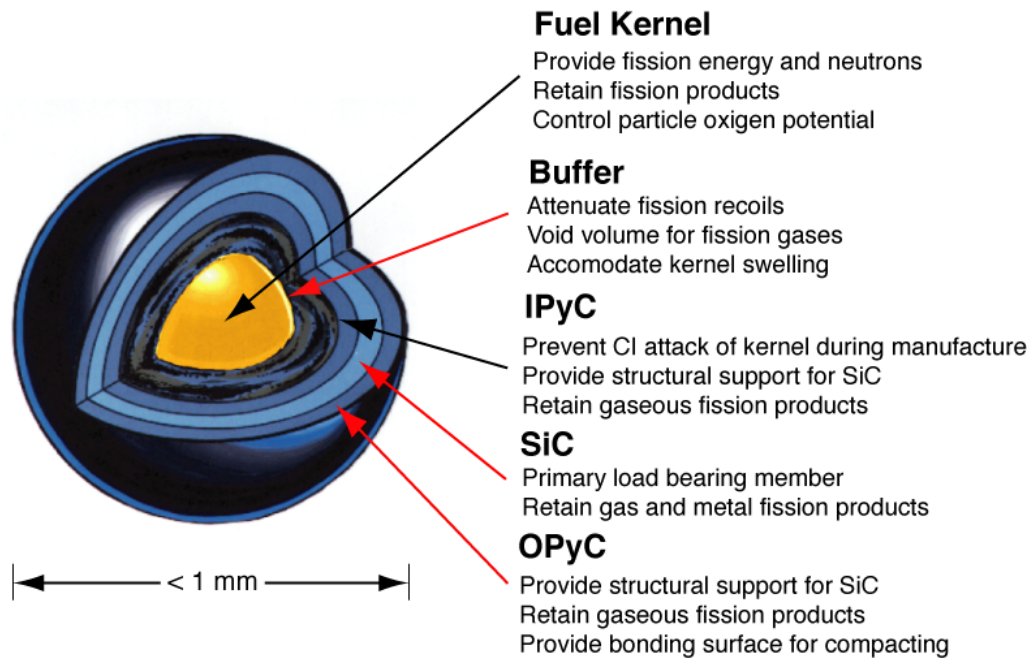


Figure 5. Parts of a TRISO particle – a miniature pressure vessel [Venneri 2005, Hanson et Saurwein 2001].

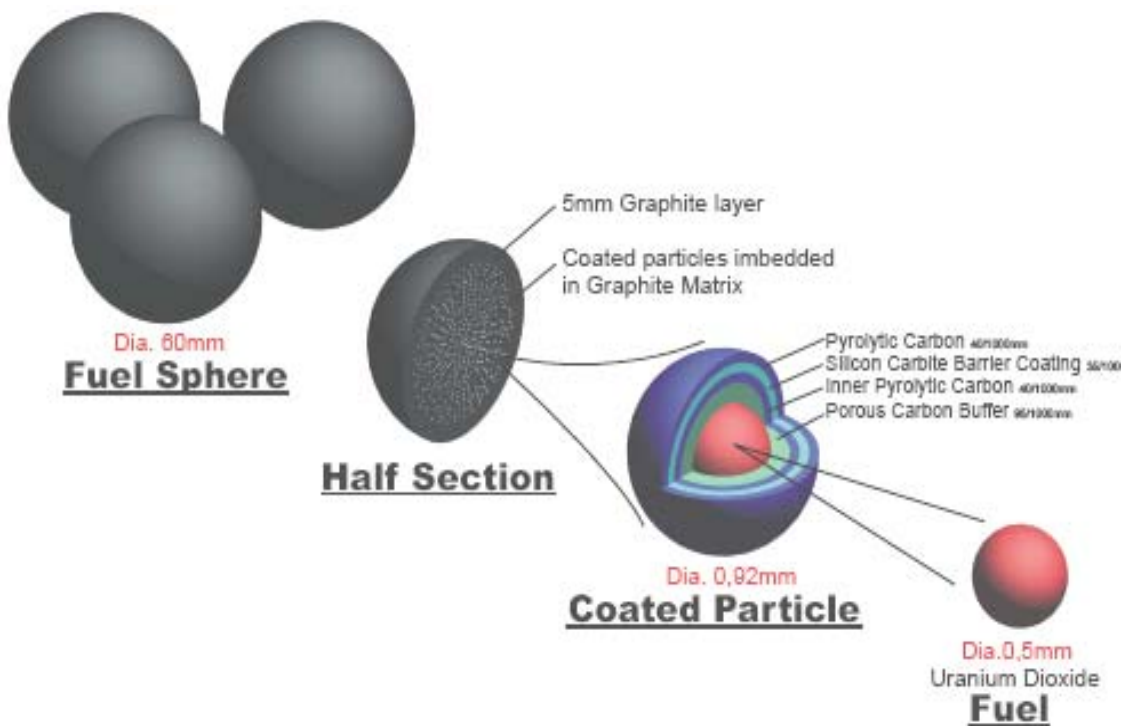


Figure 6. The base-line fuel anticipated for the South African PBMS reactor. The three coating layers and the buffer layer are designed to be a lifetime coating and encapsulation for the fuel-kernel shown in red. The aggregate fuel is shown in the two left most illustrations.



QuickTime™ and a
TIFF (Uncompressed) decompressor
are needed to see this picture.

Figure 7. Photos of the TRISO particles and cylindrical pellet, left, and the carbon prismatic fuel block for the DB-MHR, right [Hanson and Saurwein 2001].

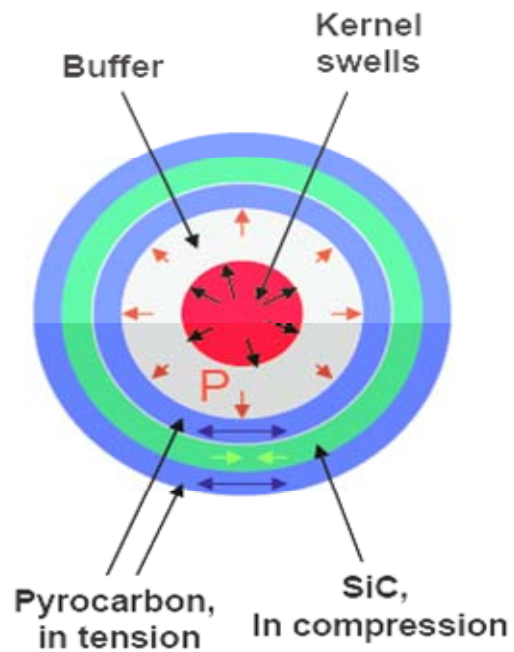


Figure 8. Mechanical forces are shown in a typical TRISO particle.

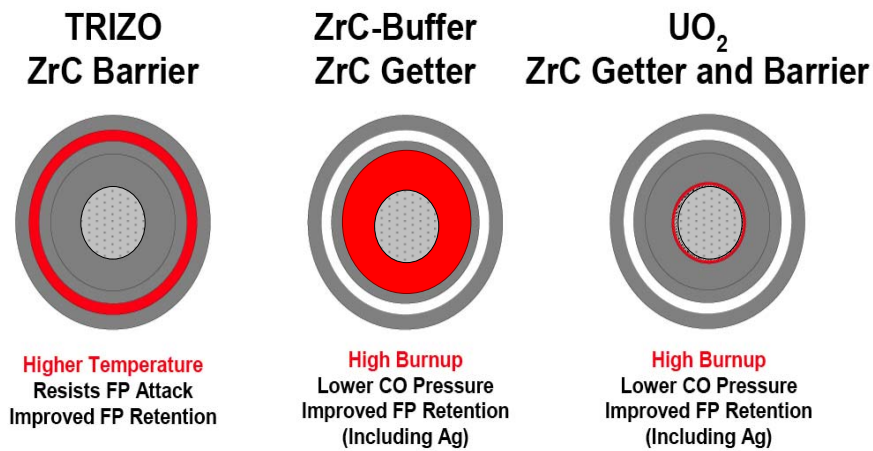


Figure 9. An example of how the use of ZrC improves TRISO deep-burn performance, left to right: replace SiC with ZrC, use as a getter in the buffer, use as a getter and barrier around the kernel.

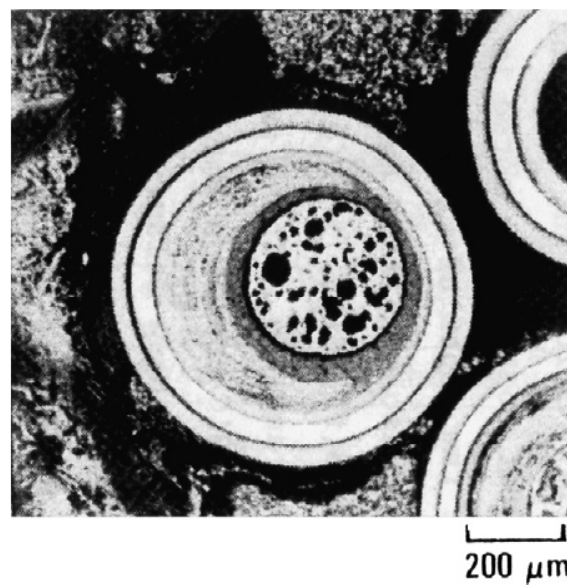


Figure 10. Migration of a UO₂ kernel in a TRISO particle [Maki et al. 2007].

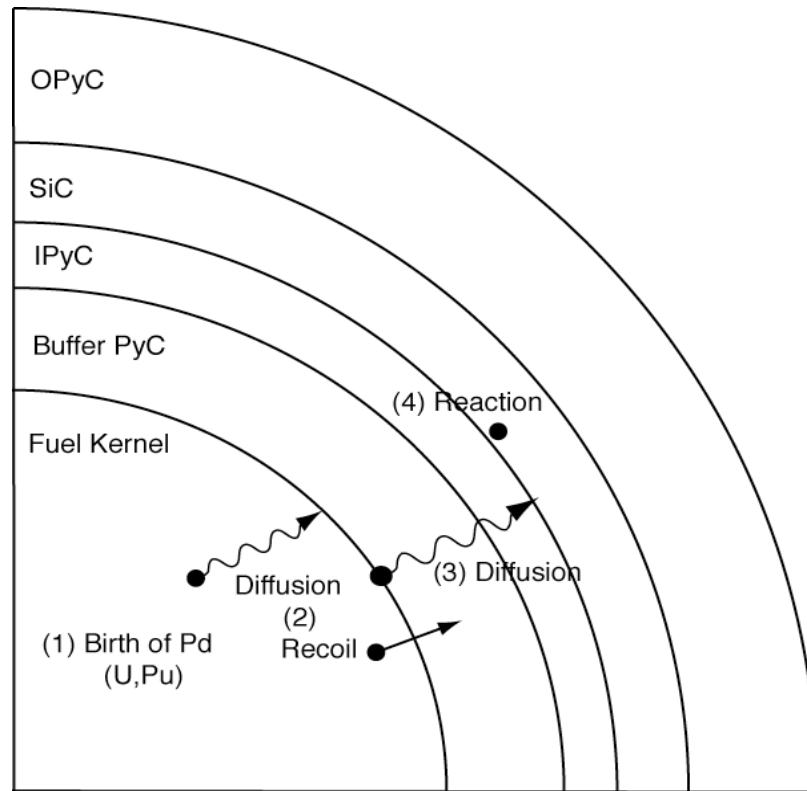


Figure 11. Schematic representation of the corrosion mechanism of the SiC layer by the FP Pd in a TRISO particle [Minato et al. 1990].

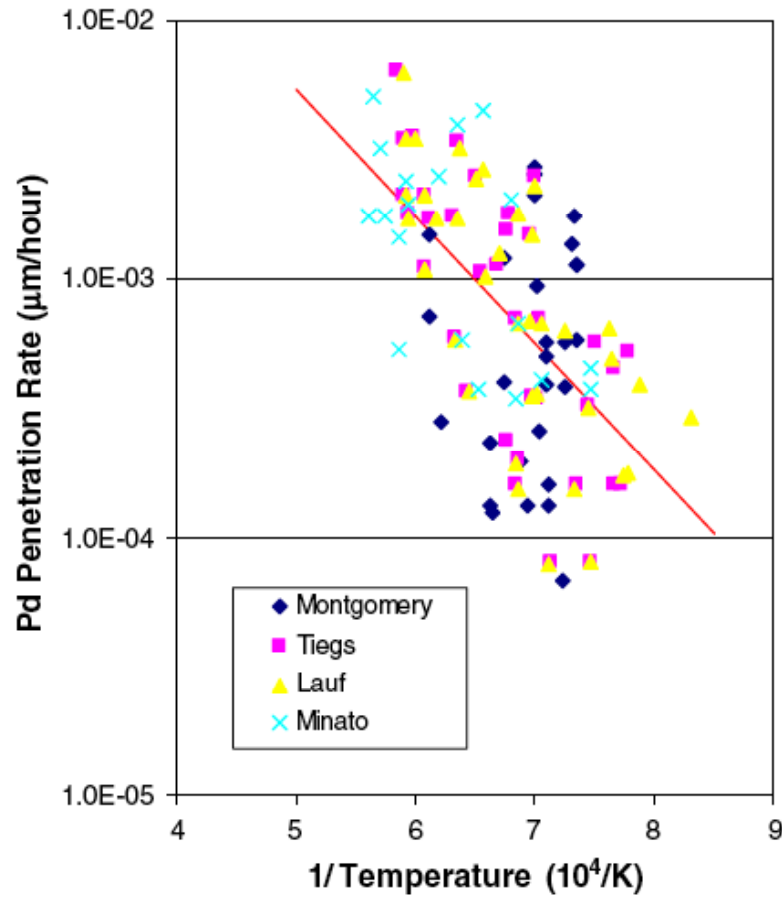


Figure 12. Pd penetration rate into SiC as a function of the inverse temperature, based on international data [Maki et al. 2007].

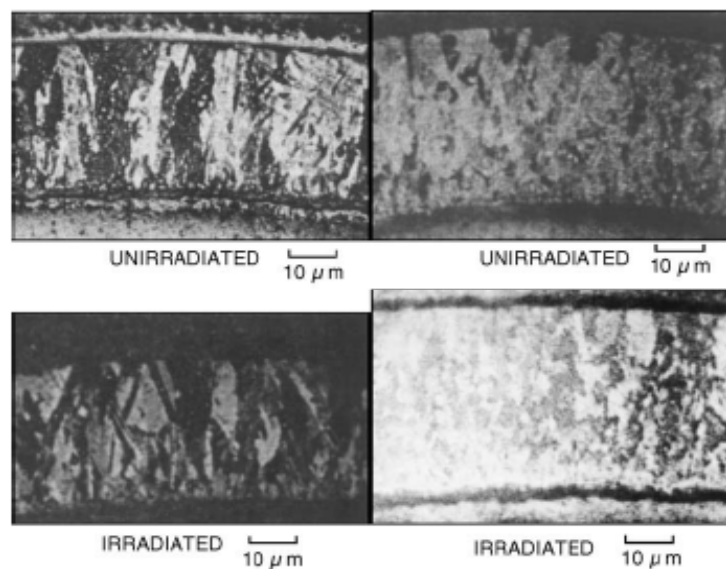


Figure 13. Photomicrographs of large thru-wall columnar SiC grains and smaller SiC grains produced in UCO fuel.

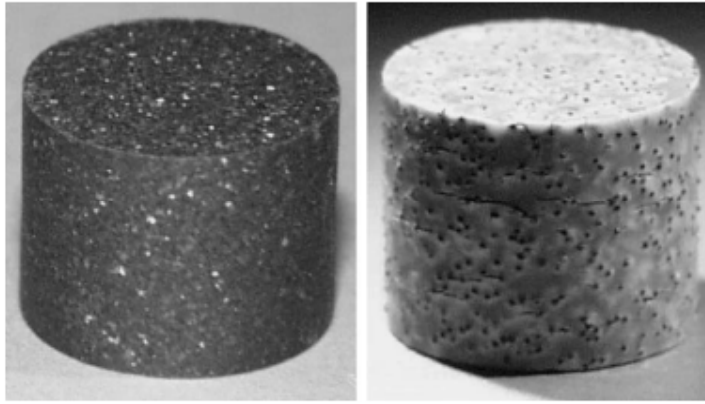


Figure 14. Examples of IMF fuel pellets. (Left) spinel based IMF with a heterogeneous micro dispersion ($<25\mu\text{m}$) and (right) spinel with heterogeneous macro-dispersion ($>100\mu\text{m}$) of fuel spheres that can be seen at the surface of the pellet.

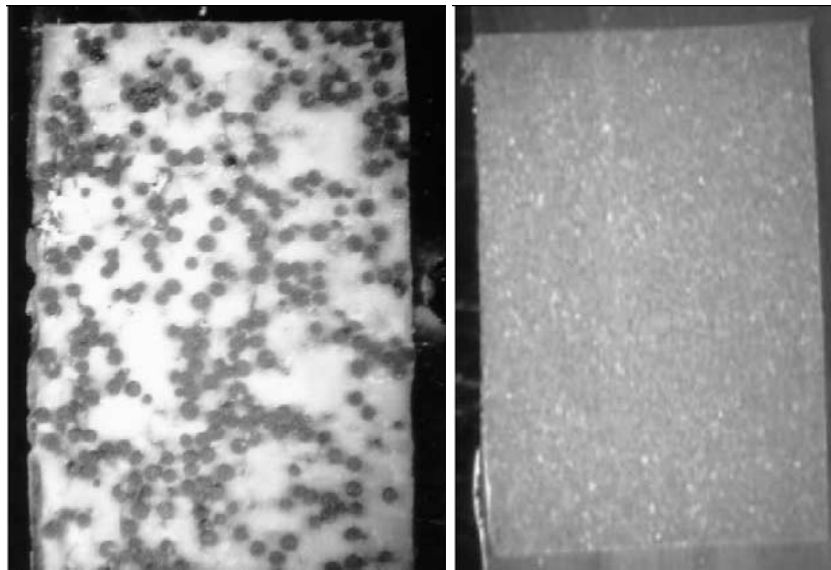


Figure 15. Examples of cross-sections of a macro-dispersed IMF (left) using microspheres $\sim 100\mu\text{m}$ Ø of fuel and a micro-dispersed IMF (right) using crushed $<25\mu\text{m}$ Ø of the same fuel microspheres.

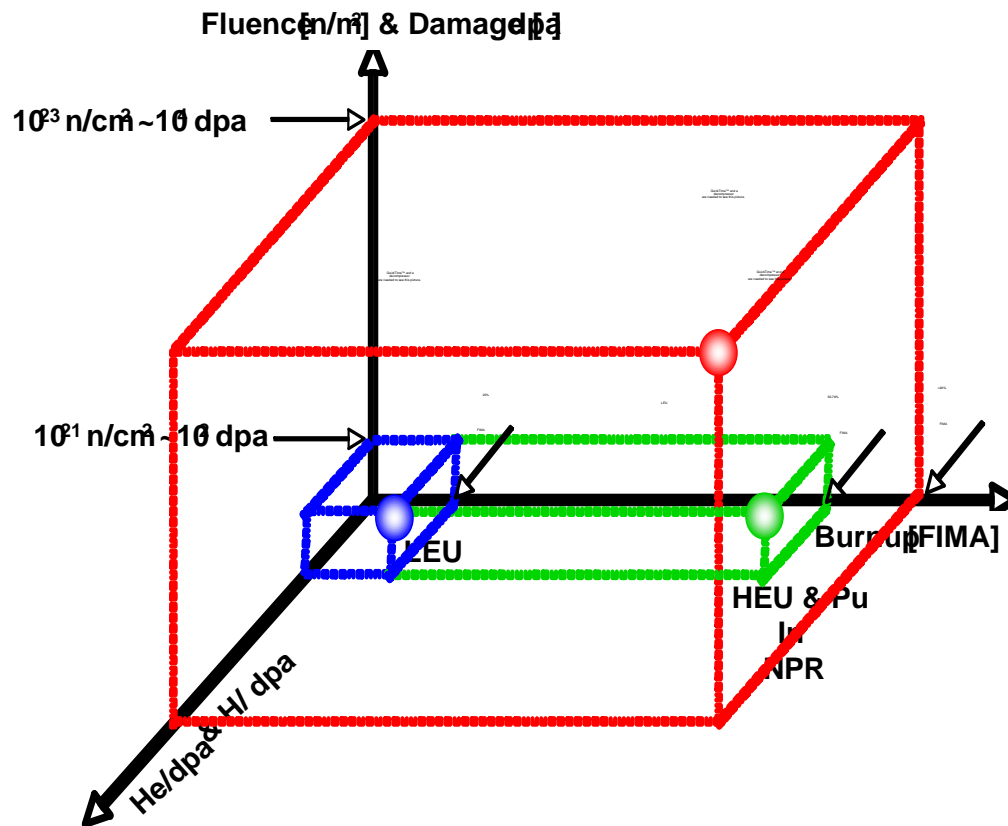


Figure 16. Three points are shown in this illustration: (blue) represents successful experience with TRISO fuels achieving FIMA of ~20% using LEU; (green) successful exploratory research with TRISO fuels burning HEU or Pu, or Pu+MA to FIMA of ~70%; and (red) represents the goal for achieving ultra-high burn-up (FIMA>90%) for LEU or NEU TRISO fuels in hybrid reactors. While high burn-up is a specific challenge because most of the fuel is FP at EOL, the radiation effects from the large neutron fluence also represents an additional challenge to the materials design.

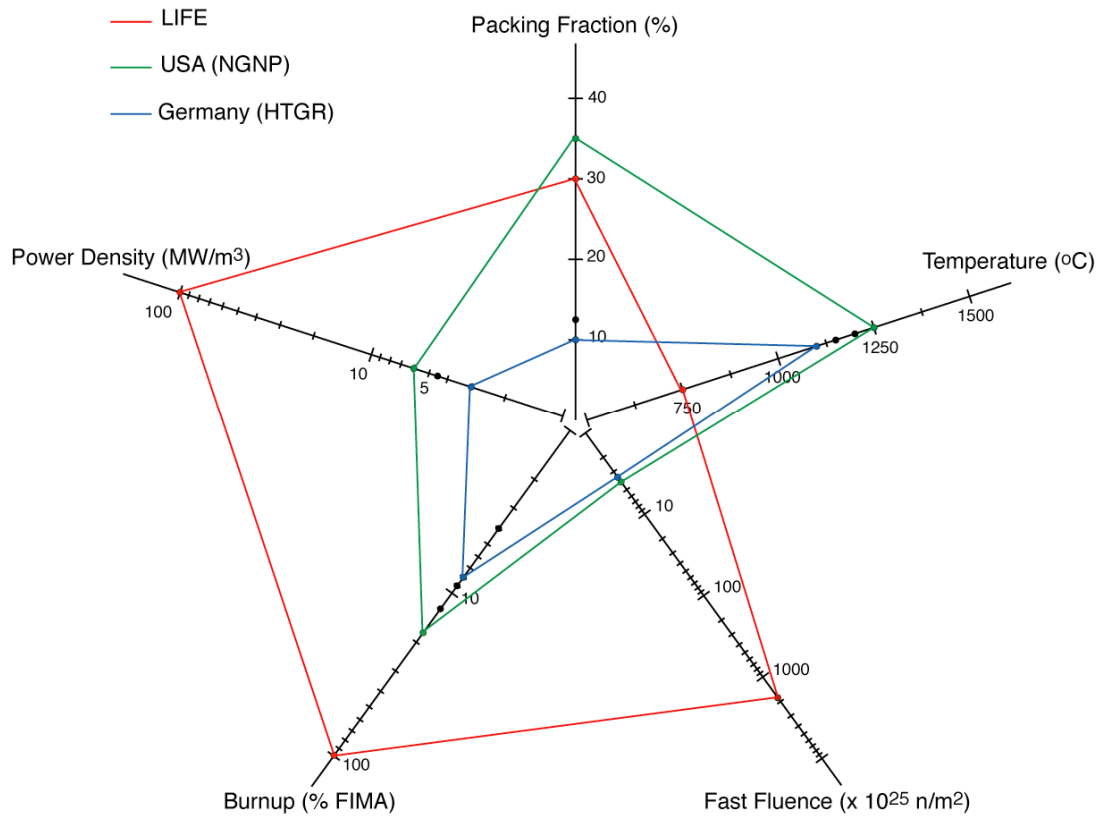


Figure 17. US VHTR and German HTGR fuels operating envelope compared with LIFE requirements [Maki et al. 2007, Latkowski 2008]. Note that power density, burn-up, and fast-fluence axes are on a log scale.

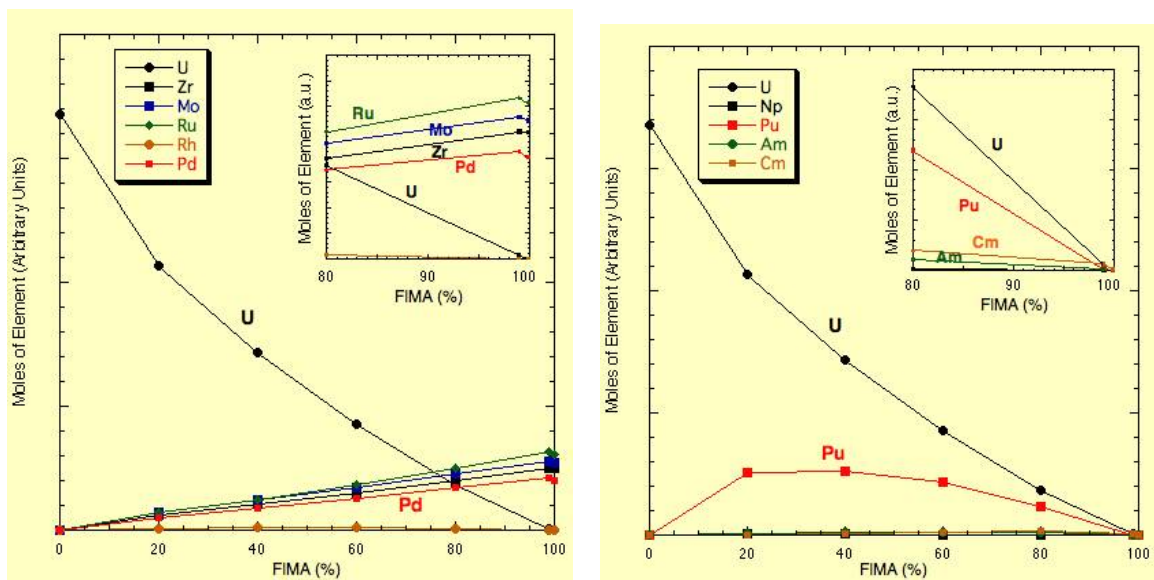


Figure 18. Evolution of fuel components with FIMA (*i.e.*, time or burn-up).

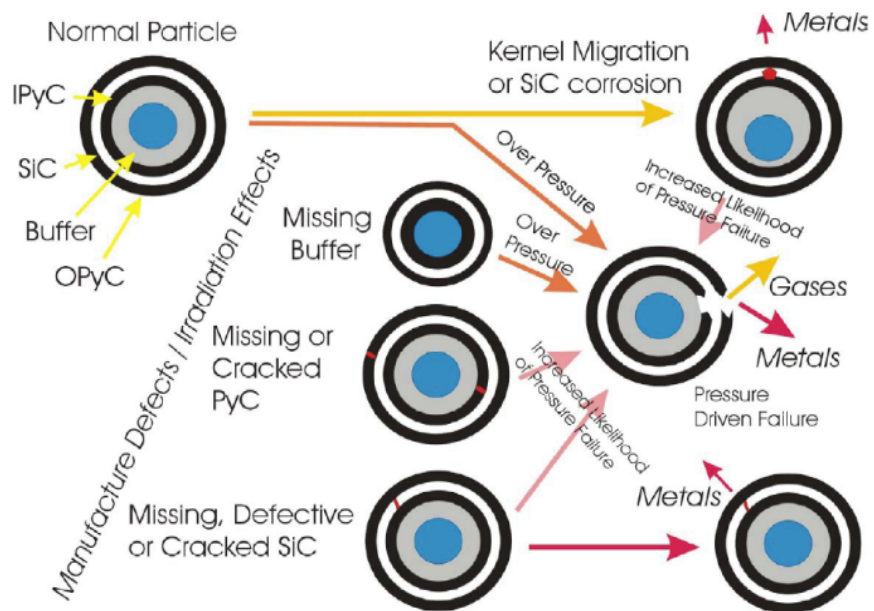


Figure 19. Failure mechanisms and their pathways for standard TRISO particles [General Atomics 2006].

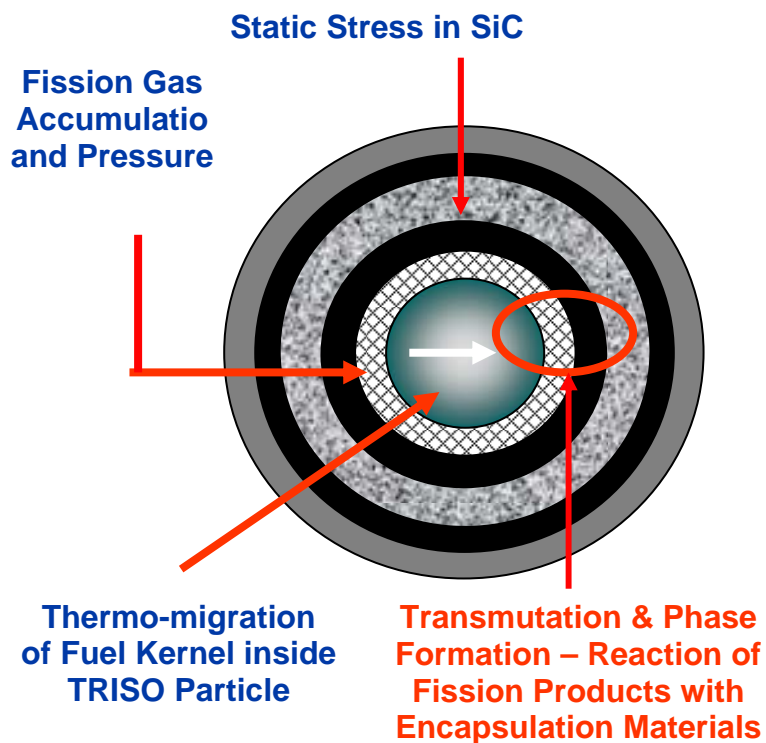


Figure 20. Main issues that affect the performance of a TRISO particle.

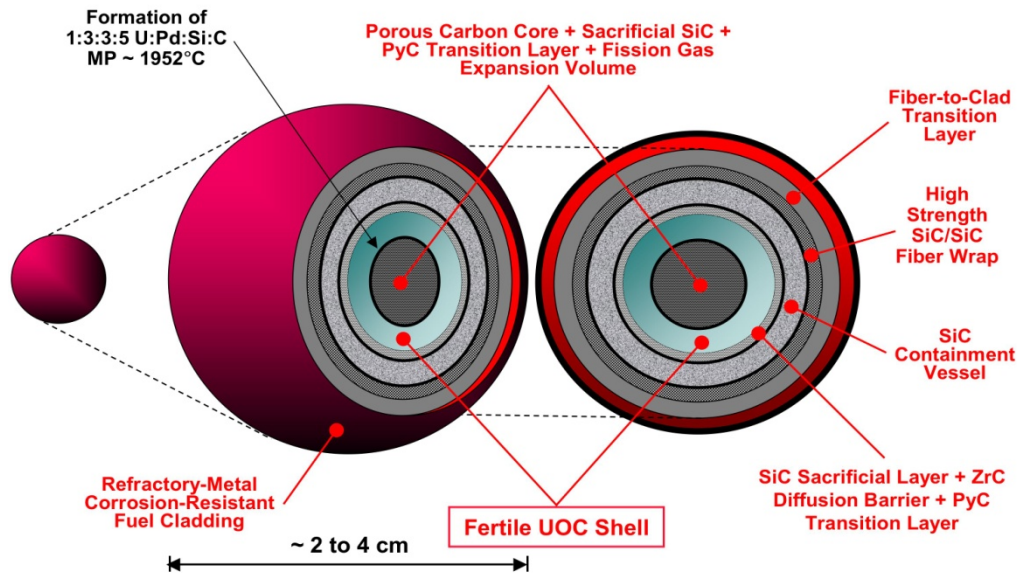


Figure 21. Schematics of a solid hollow core fuel pebble.

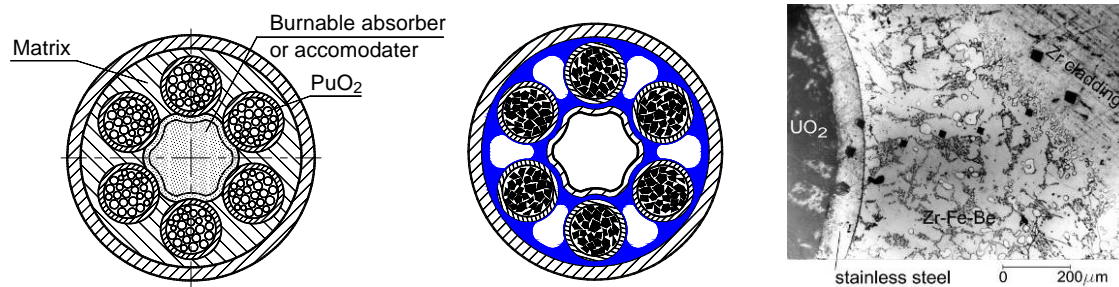


Figure 22. Schematics representation of IMF version proposed for thermal and fast reactors [Savchenko et al. 2008c, Savchenko and Konovalov 2008]. Impregnation (left), capillary impregnation (middle), and impregnation of a Zr matrix (right).

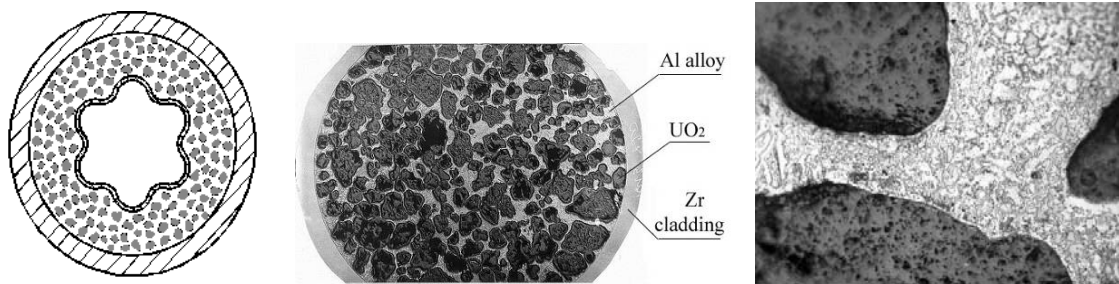


Figure 23. Schematics representation of IMF version originally proposed for thermal reactor [Savchenko et al. 2008c]. Cross section of fuel element with heterogeneous arrangement of fuel (left), microstructure of UO_2 fuel sample (middle), and microstructure of sample of heterogeneously arranged fuel element with UO_2 in a Zr-based matrix, Zr-6.2Fe-02.5Be (right) [Savchenko et al. 2006a, Savchenko et al. 2006b].

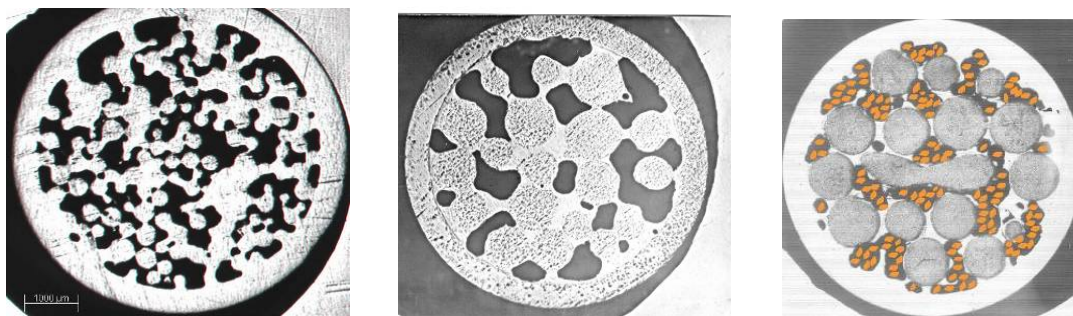


Figure 24. Schematics representation of heterogeneous fuel arrangement within the pores of a Zr-based alloy frame [Savchenko et al. 2008c]. Microstructure of Zr porous matrix fabricated by capillary impregnation from Zr powder (left), Zr granules (middle), and U- PuO_2 dispersion (with PuO_2 located schematically in the pores) [Savchenko et al. 2008c].

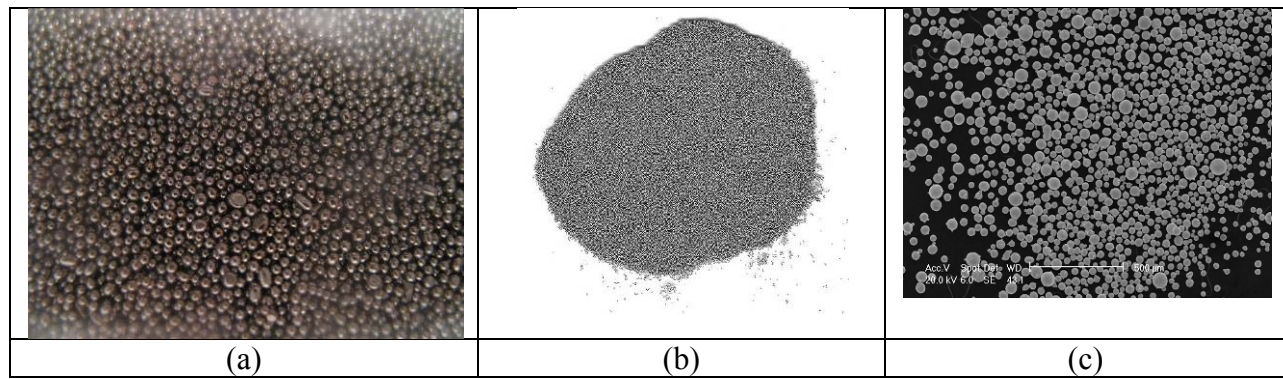


Figure 25. Appearance of the initial components of the combined U-PuO₂ fuel: (a) U-Mo alloy granules, (b) Zr-Fe-Cu alloy matrix granules, and (c) PuO₂ powder manufactured by pyro-chemical method [Savchenko et al. 2006a, Savchenko et al. 2008a].

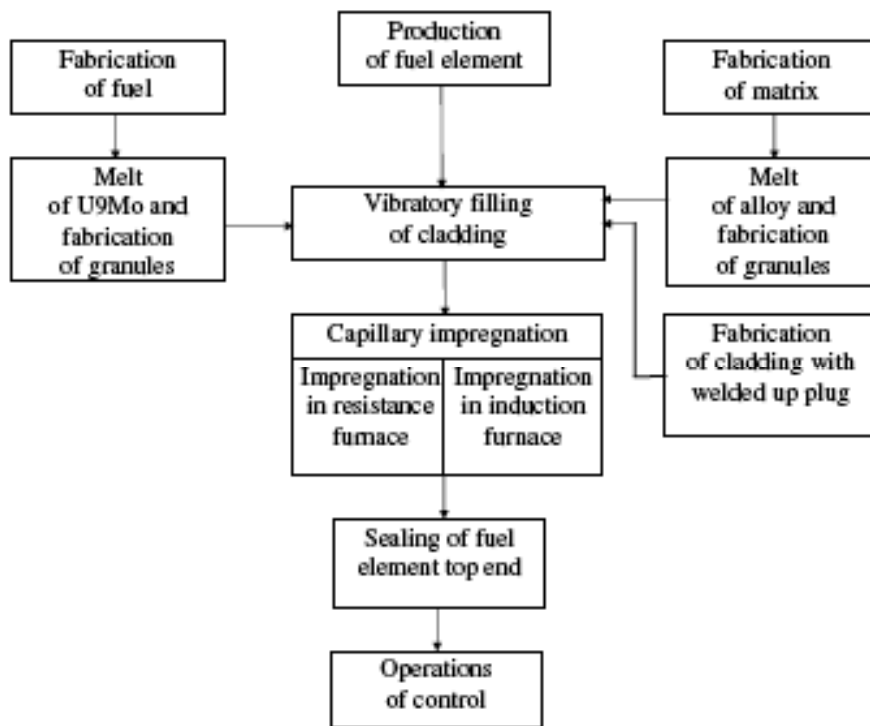


Figure 26. Example of a process-flow sheet of fuel-element fabrication by a capillary-impregnation method [Savchenko et al. 2007a].

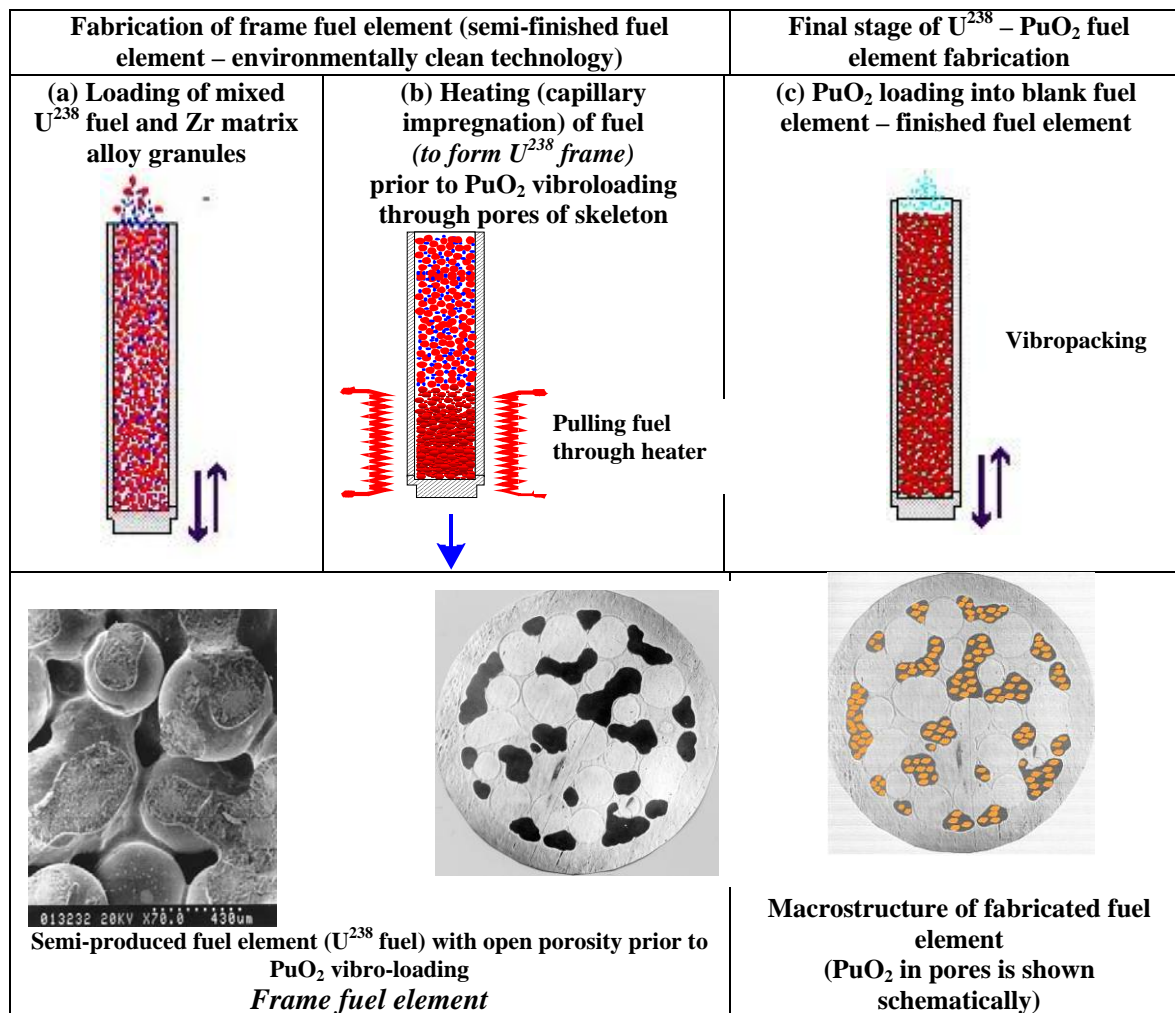


Figure 27. U- PuO_2 dispersion combined fuel, in replacement of MOX fuel, and fabrication stages [Savchenko et al. 2008a].

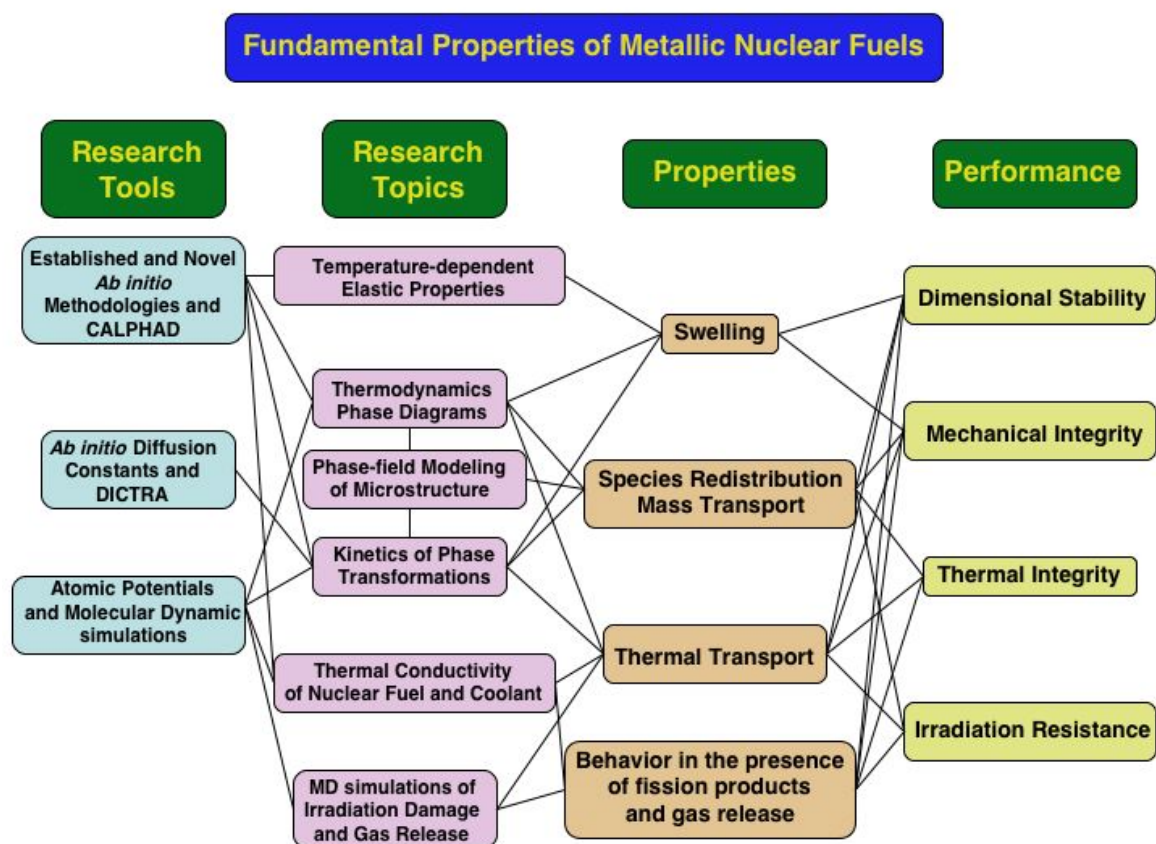


Figure 28. Flow chart describing the relations between thermodynamic and kinetic studies and properties and performance of advanced metallic nuclear fuels.

Appendix A. Thermo-Calc and CALPHAD Modeling

Thermo-Calc version R is a commercially available software code [1] that fulfills the need for critical modeling and analysis of data to:

- Produce, refine, and analyze multi-component phase diagrams of alloys at relevant temperatures for predicting phase stability properties.
- Determine the solidification path and long-term aging of alloys.
- Generate isothermal sections of multi-component alloy phase diagrams at relevant temperatures, isopleths, and property diagrams (phase fractions as functions of temperature), and composition versus temperature for all stable and metastable phases forming.
- Simulate phase transformations according to the Scheil-Gulliver model (for which local equilibria, infinite diffusion in the liquid phase, and no back diffusion in the solid phase are assumed).

Thermo-Calc is specially designed for systems with strongly non-ideal phases. It has gained a worldwide reputation as the best software application for calculation of multi-component phase diagrams. It is the only commercially available software that can calculate arbitrary phase diagram sections with up to five independent variables in multi-component systems. There are also modules to calculate many other types of properties, such as, Scheil-Gulliver solidification simulations, Pourbaix diagrams, partial pressures in gases, and more.

In the CALPHAD approach [2-5], the Gibbs energy of individual phases is modeled, and the model parameters are collected in a thermodynamic database. It is the modeling of the Gibbs energy of individual phases and the coupling of phase diagram and thermo-chemistry that make the CALPHAD a powerful technique in computational thermodynamics of multi-component materials. Models for the Gibbs energy are based on the crystal structures of the phases. For pure elements and stoichiometric compounds, the most commonly used model is the one suggested by the Scientific Group Thermodata Europe (SGTE) [6] and has the following form (for simplicity, the pressure dependence and the magnetic contribution are not shown here),

$$G_m - H_m^{SER} = a + bT + cT \ln(T) + \sum d_i T^i \quad (A.1)$$

The left-hand side of Eq. A.1 is defined as the Gibbs energy relative to a standard element reference state (SER), where H_m^{SER} is the enthalpy of the element in its stable state at 298.15 K and 1 bar of pressure. Coefficients, a, b, c, and d_i are the model parameters. The SGTE data for all the pure elements of the periodic table have been compiled by Dinsdale [6].

For multi-component solution phases, the Gibbs energy has the following general expression [3-5],

$$G = G^o + G_{mix}^{ideal} + G_{mix}^{xs} \quad (A.2)$$

where G^o is the contribution from the mechanical mixing of the pure components, G_{mix}^{ideal} is the ideal mixing contribution, and G_{mix}^{xs} is the excess Gibbs energy of mixing due to non-ideal interactions. Sublattice models have been widely used to describe solution phases [3,4]. For example, for a simple phase with two sublattices in an A-B binary system where the two components enter both sublattices, the sublattice model is written as $(A,B)_p(A,B)_q$, where subscripts p and q denote the number of sites of each sublattice. More specifically, the three terms in Eq. A.2 are written as,

$$G^o = y_A^I y_A^{II} G_{A:A}^o + y_A^I y_B^{II} G_{A:B}^o + y_B^I y_A^{II} G_{B:A}^o + y_B^I y_B^{II} G_{B:B}^o \quad (A.3)$$

$$G_{\text{mix}}^{\text{ideal}} = pRT \left(y_A^I \ln y_A^I + y_B^I \ln y_B^I \right) + qRT \left(y_A^{II} \ln y_A^{II} + y_B^{II} \ln y_B^{II} \right) \quad (A.4)$$

$$G_{\text{mix}}^{\text{xs}} = y_A^I y_B^I \left(y_A^{II} \sum_{k=0}^L L_{A:B:A}^k (y_A^I - y_B^I)^k + y_B^{II} \sum_{k=0}^L L_{A:B:B}^k (y_A^I - y_B^I)^k \right) \\ + y_A^{II} y_B^{II} \left(y_A^I \sum_{k=0}^L L_{A:A,B}^k (y_A^{II} - y_B^{II})^k + y_B^I \sum_{k=0}^L L_{B:A,B}^k (y_A^{II} - y_B^{II})^k \right) \quad (A.5)$$

where y^I and y^{II} are the site fractions of A or B in the first and second sublattices, respectively.

$G_{I,J}^o$ is the Gibbs energy of the compound $I_p J_q$, expressed by Eq. A.1. $L_{A,B}^k$ ($L_{*,A,B}^k$) is the k^{th} order interaction parameter between component A and B in the first (second) sublattice. In this notation, a colon separates components occupying different sublattices, and a comma separates interacting components in the same sublattice. These equations can be generalized for phases with multi-components and multi-sublattices, and they reduce to a random substitutional model when there is only one sublattice.

For a multi-component solution in a particular phase \square described with a single sublattice model, the three contributions to the total Gibbs energy reduce to [3,4]:

$$\Phi G^o = \sum_I c_I \Phi G_I^o \\ \Phi G_{\text{mix}}^{\text{ideal}} = RT \sum_I c_I \ln c_I \quad (A.6)$$

$$\Phi G_{\text{mix}}^{\text{xs}} = \sum_I \sum_{J>I} c_I c_J \sum_k \Phi L_{I,J}^k (c_I - c_J)^k$$

where the molar Gibbs energy of mixing is expressed by a Redlich-Kister expansion [7]. In these expressions c_I is the composition of the alloy in species I, and the $L_{I,J}^k$ is the k^{th} -order binary interaction parameter between species I and J expressed as a polynomial in temperature T. Note that in both sets of expressions the excess Gibbs energy due to non-ideal contributions is expressed within the Muggianu approximation [8].

Finally for stoichiometric compounds, the Gibbs energy only depends on temperature and is simply given by

$${}^{\text{Comp}}G(T) = {}^{\text{Comp}}G^0(T) - \sum_I c_I H_I^{\text{SER}}(298.15 \text{ K}) \\ \approx a + bT + \sum_I c_I \left[\Phi_I G_I^0(T) - H_I^{\text{SER}}(298.15 \text{ K}) \right] \quad (A.7)$$

Data generated with the Thermo-Calc software also provide the basis for more accurate predictions of diffusion kinetics and ultimately TTT (temperature-time-transformations) diagrams with the DICTRA software [1] by assuming diffusion both in the liquid and the solid phase. Note that the results of both equilibrium solidification and Scheil-Gulliver simulations generated by Thermo-Calc correspond to upper and lower bounds for the DICTRA results.

Input thermodynamic data files used by Thermo-Calc are: KP (Kaufman binary alloys database), SSOL (Scientific Group Thermodata Europe, or SGTE, solution database), from published journals, and/or from qualified sources. Here to describe the alloy systems that are relevant for addressing phase formation and transformations in solid fuels, and stability of molten salts in the

presence of fissile and fertile nuclear fuels and fission products, a thermodynamic database was developed based on available data on phase diagrams from relevant literature [9,10].

References

- [1] The Thermo-Calc and DICTRA applications software are products of Thermo-Calc AB; B. Sundman, B. Jansson, and J.-O. Andersson, “The Thermo-Calc Databank System”, *CALPHAD* **9** (4), 153 (1985); J.-O. Andersson, T. Helander, L. Höglund, Pingfang Shi, and B. Sundman, “THERMO-CALC & DICTRA, computational tools for materials science”, *CALPHAD* **26** (2), 273-312 (2002); cf. also <http://www.thermocalc.se>.
- [2] L. Kaufman and H. Bernstein, “Computer Calculation of Phase Diagrams with Special Reference to Refractory Metals” (Academic Press, New York, 1970).
- [3] N. Saunders and A. P. Miodownik, “*CALPHAD, Calculation of Phase Diagrams: A Comprehensive Guide*”, Pergamon Press (1998).
- [4] “*CALPHAD and Alloy Thermodynamics*”, ed. by P. E. A. Turchi, A. Gonis, and R. D. Shull (TMS Publication, Warrendale, PA, 2002); and references therein.
- [5] MRS Bulletin, Vol. 24, No. 4 (April 1999), “Computer Simulations from Thermodynamic Data: Materials Production and Development”, p. 18-49.
- [6] A. Dinsdale, “SGTE Database for Pure Elements”, *CALPHAD* **15**, 317-425 (1991).
- [7] O. Redlich and A. Kister, “Algebraic Representation of the Thermodynamic Properties and the Classification of Solutions”, *Ind. Eng. Chem.* **40**, 345-348 (1948).
- [8] Y. M. Muggianu, M. Gambino, and J. P. Bros, “Enthalpies de Formation des Alliages Liquides Bismuth-Etain-Gallium à 723 K. Choix d’une Représentation Analytique des Grandeurs d’Excès Intégrales et Partielles de Mélange”, *J. Chem. Phys.* **22**, 83-88 (1975).
- [9] T. B. Massalski, ed., “*Handbook of Alloy Phase Diagrams*”, 3 volumes, ASM Materials Park, Ohio (1990).
- [10] “*Phase Diagram of Binary Actinide Alloys*”, Monograph Series on Alloy Phase Diagrams, vol. 11, M. E. Kassner and D. E. Peterson eds. (ASM International, Materials Park, OH, 1995).

Appendix B. Thermodynamic Database for Solid Fuel Modeling

It is anticipated that the evolution of fuel composition with burn-up (or FIMA) will have important consequences on materials performance. Therefore, compatibility issues between fuel materials and their surrounding will have to be addressed, especially because of the wide range of FP that will form as a function of time. The fuel integrity will be affected by phenomena such as kernel migration, amoeba effect, limited solubility, low melting of protective layers, and precipitation of deleterious phases. These phenomena will consequently affect the mechanical integrity of the fuel particle (*e.g.*, stress swelling, cracking, etc.). Hence, it is important to gain a fundamental knowledge on the thermodynamic properties of complex multi-component mixtures, the composition of which evolves with time. In addition, the thermo-mechanical behavior of fuel particles is function of CO, CO₂, and FG release whose gas pressures must be well known to calculate the stresses. In addition, the chemical state of the FP and their diffusion coefficients that influence thermal conductivity, creep, and melting point of the fuel must be determined. Also, to account for the role of FP on CO and CO₂ release, and to understand, control, and predict the chemical interactions in the irradiated fuel particle and the escape of FP from a defective fuel under normal and accidental conditions, the thermodynamic properties of all gas, liquid, and solid phases, and the associated phase diagrams of these complex system, fuel particle + FP, have to be assessed.

As a first step towards this goal, an effort has been put in developing a fully V&V thermodynamic database that includes the following elements: C, O, Pd, Pu, Si, U, and Zr. The status of this database is given in Table B.1, together with the references to the data that are available in the literature. This database will be used to address issues on solid fuels, and will serve as input to kinetic studies for predicting the time evolution of fuel phases under LIFE conditions, in the case of the three main options that have discussed in the body of the report, *i.e.*, TRISO, SHC and IMF. Note that a similar activity has been initiated to address the specific issues raised in the case of molten salt fuels.

	C	O	Pd	Pu	Si	U	Zr
C							
O							
Pd							
Pu							
Si							
U							
Zr							

Table B.1. Current status of the thermodynamic database under development for solid fuels. In red are the binary combinations that have been fully assessed and validated by experimental data.

To address several important and immediate issues, and in particular the Pd attack in TRISO particle, an interim thermodynamic database that is not fully validated has been put in place. The status of this database is given in Table B.2. Note that for this database, the number of binaries

(ternaries) that need to be thermodynamically assessed has been reduced to 15 (20), compared with 21 (35), for the V&V database given in Table B.1

	C	O	Pd	Si	U	Zr
C						
O						
Pd						
Si						
U						
Zr						

Table B.2. Interim thermodynamic database for solid fuels. In red are the binary combinations that have been thermodynamic described.

In the case of the V&V thermodynamic database given in Table B.1, there is a need to describe the following binaries, and validate, whenever experimental data are available, the ternary combinations of alloy species. In Figs. B.1-3 a sample of the binary phase diagrams that have been fully thermodynamically assessed so far are shown. These phase diagrams and the thermodynamic data on which they are based are in excellent agreement with experimentally available data.

It is worth noting that although most of the binaries that are relevant for studying the thermodynamic properties of solid nuclear fuels are available in the literature, the bulk of the effort needs to concentrate on making the thermodynamic models on which the thermodynamics of the binary combinations relies on fully compatible before multi-component materials can be examined.

A thorough compilation of existing thermodynamic data that were used to develop a consistent V&V thermodynamic database with, initially the seven elements selected in Table B.1 is presented in the following. Some additional elements have been included in the compilation since it is anticipated that future investigations will require this thermodynamic information.

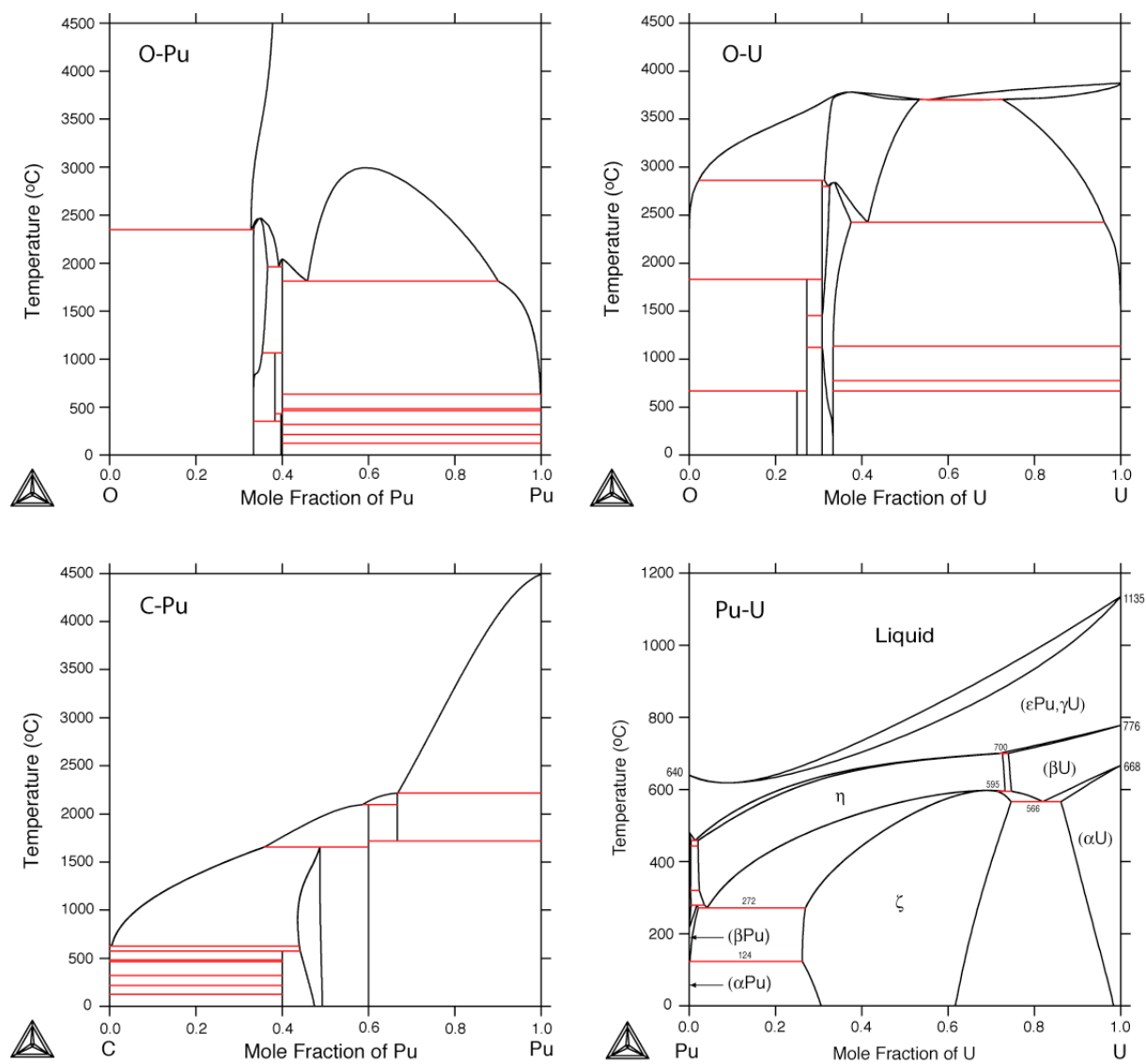


Figure B.1. CALPHAD assessment results of the O-U, O-U, C-Pu, and Pu-U binary phase diagrams.

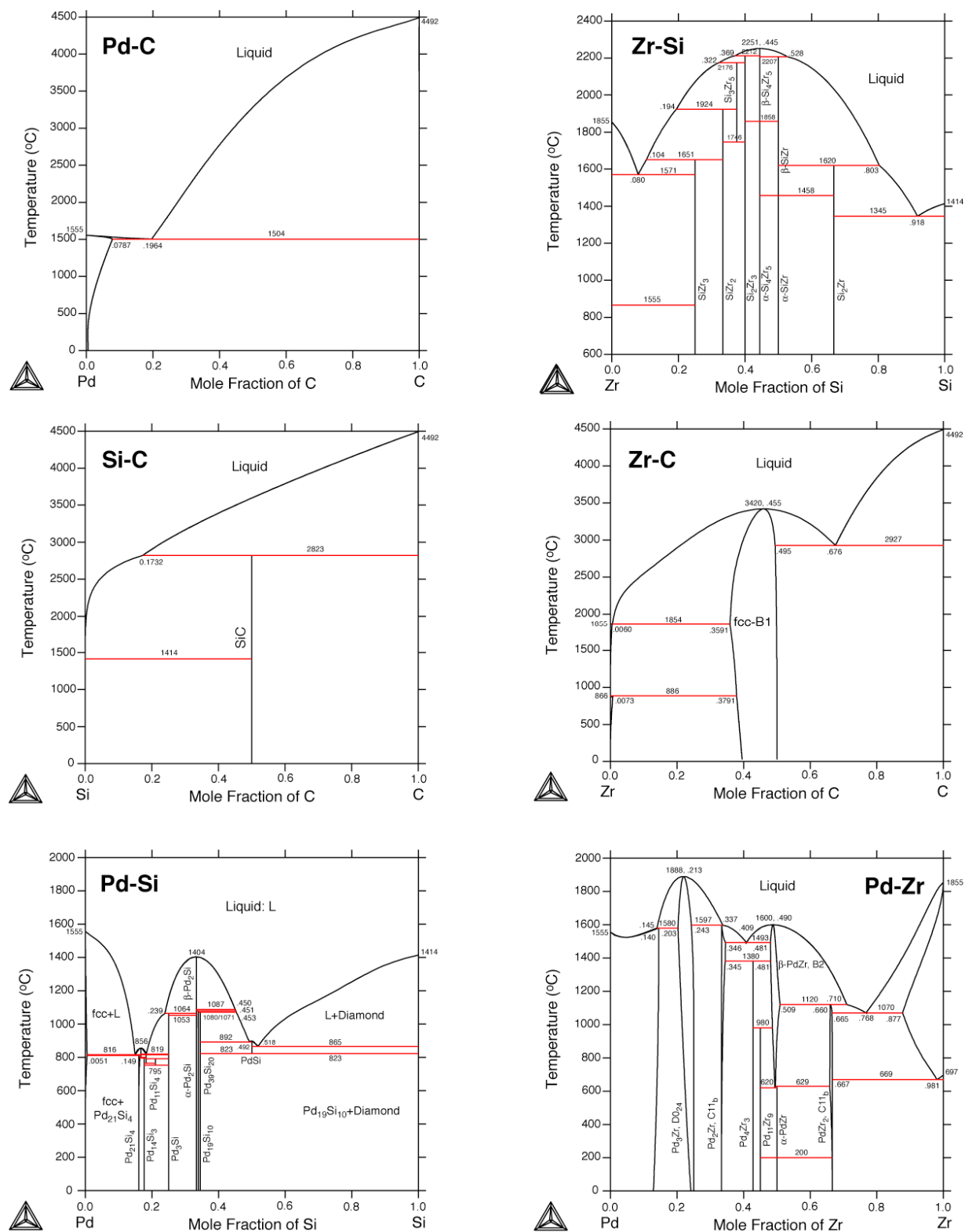


Figure B.2. CALPHAD assessment results of the Pd-C, Si-C, Pd-Si, Zr-Si, Zr-C, and Pd-Zr binary phase diagrams.

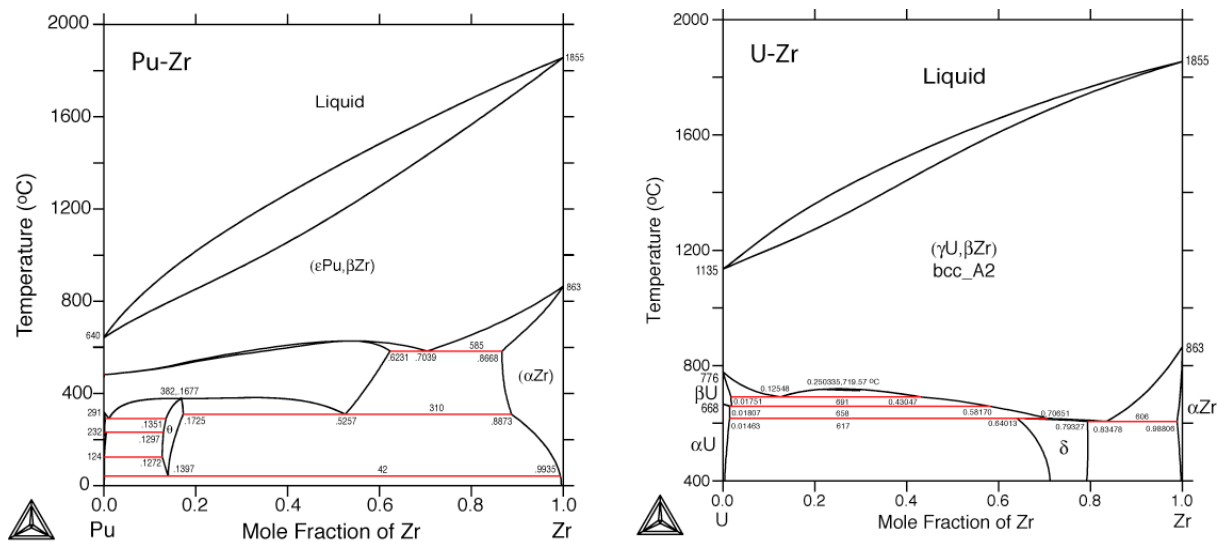


Figure B.3. CALPHAD assessment results of the Pu-Zr and U-Zr binary phase diagrams.

Based on the 7 elements indicated in Table B.1, 21 binaries need to be fully assessed, and among the 35 ternary systems, the most important ones have been confirmed experimentally in some (if not in the entire) alloy composition field and will be used to validate the CALPHAD predictions.

Binaries (21)

C-O – C-Pd – C-Pu – C-Si – C-U – C-Zr

O-Pd – O-Pu – O-Si – O-U – O-Zr

Pd-Pu – Pd-Si – Pd-U – Pd-Zr

Pu-Si – Pu-U – Pu-Zr

Si-U – Si-Zr

U-Zr

Ternaries (35)

C-O-Pd – C-O-Pu – C-O-Si – C-O-U – C-O-Zr

C-Pd-Pu – C-Pd-Si – C-Pd-U – C-Pd-Zr

C-Pu-Si – C-Pu-U – C-Pu-Zr

C-Si-U – C-Si-Zr

C-U-Zr

O-Pd-Pu – O-Pd-Si – O-Pd-U – O-Pd-Zr

O-Pu-Si – **O-Pu-U** – O-Pu-Zr

O-Si-U – O-Si-Zr

O-U-Zr

Pd-Pu-Si – Pd-Pu-U – Pd-Pu-Zr

Pd-Si-U – Pd-Si-Zr

Pd-U-Zr

Pu-Si-U – Pu-Si-Zr

Pu-U-Zr

Si-U-Zr

References – Binary Alloys

C-Pu

Evelyn Fischer, “Thermodynamic modeling of the C-Pu binary system”, CALPHAD **32**, 371-377(2008).

C-U

P. Y. Chevalier and E. Fischer, “Thermodynamic modeling of the C-U and B-U binary systems”, J of Nucl. Mater. **288**, 100-129 (2001).

Chandra Bhanu Basak, “Classical molecular dynamics simulation of uranium monocarbide (UC)”, Comput. Mater. Science **40**, 562-568 (2007).

J. Laugier and P. L. Blum, “Le diagramme metastable UC-UC₂”, J. of Nucl. Mater. **39**, 245-252 (1971).

O-Pu

H. Kinoshita, M. Uno, and S. Yamanaka, “Phase relation assessment of the O-Pu-Zr system by thermodynamic modeling”, J. of Alloys and Compounds **353**, 129-137 (2003).

R. G. Haire and J. M. Haschke, “Plutonium oxide systems and related corrosion products”, MRS Bulletin, vol. **26**, No. 9, 689-696 (2001).

Theodore M. Besmann and Terrence B. Lindemer, “Chemical thermodynamic representations of <PuO_{2-x}> and <U_{1-z}Pu_zO_w>”, J. of Nucl. Mater. **130**, 489-504 (1985).

Han Soo Kim, Chang Yong Joung, Byung Ho Lee, Jae Yong Oh, Yang Hyun Koo, Peter Heimgartner, “Applicability of CeO₂ as a surrogate for PuO₂ in a MOX fuel development”, J. of Nucl. Mater. **378**, 98-104 (2008).

Christine Guéneau, Christian Chatillon, and Bo Sundman, “Thermodynamic modelling of the plutonium–oxygen system”, J. of Nucl. Mater. **378**, 257-272 (2008). (doi:10.1016/j.jnucmat.2008.06.013)

V. Sobolev, “Modelling thermal properties of actinide dioxide fuels”, J. of Nucl. Mater. **344**, 198-205 (2005).

O-U

M. Barrachin, P.Y. Chevalier, B. Cheynet, and E. Fischer, “New modelling of the U-O-Zr phase diagram in the hyperstoichiometric region and consequences for the fuel rod liquefaction in oxidising conditions”, J. of Nucl. Mater. 2008.

C. Guéneau, M. Baichi, D. Labroche, C. Chatillon, and B. Sundman, “Thermodynamic assessment of the uranium-oxygen system”, J. of Nucl. Mater. **304**, 161-175 (2002).

P. Y. Chevalier, E. Fischer, and B. Cheynet, “Progress in the thermodynamic modeling of the O-U-Zr ternary system”, CALPHAD **28**, 15-40 (2004); and references therein.

P. Y. Chevalier, E. Fischer, and B. Cheynet, “Progress in the thermodynamic modeling of the O-U binary system”, J. of Nucl. Mater. **303** (1), 1-28 (2002).

P. Y. Chevalier and E. Fischer, “Thermodynamic modelling of the O-U-Zr system”, J. of Nucl. Mater. **257**, 213-255 (1998).

M. Freyss, T. Petit, J.-P. Crocombette, “Point defects in uranium dioxide: Ab initio pseudopotential approach in the generalized gradient approximation”, J. of Nucl. Mater. **347**, 44-51 (2005).

M. Baichi, C. Chatillon, G. Ducros, and K. Froment, “Thermodynamic of the O-U system: III – Critical assessment of phase diagram data in the U-UO_{2+x} composition range”, J. of Nucl. Mater. **349**, 57-82 (2006).

M. Baichi, C. Chatillon, G. Ducros, and K. Froment, “Thermodynamic of the O-U system: IV – Critical assessment of chemical potentials in the U-UO_{2.01} composition range”, J. of Nucl. Mater. **349**, 17-56 (2006).

D. Manara, C. Ronchi, M. Sheindlin, and R. Konings, “On the present state of investigation of

thermodynamic properties of solid and liquid UO_{2+x} ”, J. of Nucl. Mater. **362**, 14-18 (2007).

K. Govers, S. Lemehov, M. Hou, M. Verwerft, “Comparison of interatomic potentials for UO_2 . Part I: Static calculations”, J. of Nucl. Mater. **366**, 161–177 (2007).

Akio Nakamura and Takeo Fujino, “Thermodynamic model of UO_{2+x} ”, J. of Nucl. Mater. **167**, 36-46 (1989).

J.D. Higgs, W.T. Thompson, B.J. Lewis, S.C. Vogel, “Kinetics of precipitation of U_4O_9 from hyperstoichiometric UO_{2+x} ”, J. of Nucl. Mater. **366**, 297-305 (2007).

Terrence B. Lindemer and Theodore M. Besmann, “Chemical thermodynamic representation of $\langle \text{UO}_{2\pm x} \rangle$ ”, J. of Nucl. Mater. **130**, 473-488 (1985).

Madiba Saidy, William H. Hocking, Jozef F. Mouris, Philippe Garcia, Gaëlle Carlot, and Bertrand Pasquet, “Thermal diffusion of iodine in UO_2 and UO_{2+x} ”, J. of Nucl. Mater. **372**, 405-415 (2008).

Taku Watanabe, Susan B. Sinnott, James S. Tulenko, Robin W. Grimes, Patrick K. Schelling, and Simon R. Phillpot, “Thermal transport properties of uranium dioxide by molecular dynamics simulations”, J. of Nucl. Mater. **375**, 388-396 (2008).

F.N. Skomurski, L.C. Shuller, R.C. Ewing, and U. Becker, “Corrosion of UO_2 and ThO_2 : A quantum-mechanical investigation”, J. of Nucl. Mater. **375**, 290-310 (2008).

M.S. Veshchunov and V.E. Shestak, “An advanced model for intragranular bubble diffusivity in irradiated UO_2 fuel”, J. of Nucl. Mater. **376**, 174-180 (2008).

Hua Y. Geng, Ying Chen, Yasunori Kaneta, and Motoyasu Kinoshita, “Stability mechanism of cuboctahedral clusters in UO_{2+x} : First-principles calculations”, Phys. Rev. **B 77**, 18101(R)-1 to 4 (2008).

Prabhathasree Goel, N. Choudhury, and S.L. Chaplot, “Atomistic modeling of the vibrational and thermodynamic properties of uranium dioxide, UO_2 ”, J. of Nucl. Mater. **377**, 438-443 (2008).

Younsuk Yun, Hanchul Kim, Heemoon Kim, and Kwangheon Park, “Atomic diffusion mechanism of Xe in UO_2 ”, J. of Nucl. Mater. **378**, 40-44 (2008).

J.-P. Hiernaut, P. Gotcu, J.-Y. Colle, and R.J.M. Konings, “Thermodynamic study of actinides and lanthanides during total vaporization of a very high burn-up UO_2 fuel”, J. of Nucl. Mater. **378**, 349-357 (2008).

Tapan G. Desai, Paul C. Millett, and Dieter Wolf, “Molecular dynamics study of diffusional creep in nanocrystalline UO_2 ”, Acta Materialia **56**, 4489-4497 (2008).

V. Sobolev, “Modelling thermal properties of actinide dioxide fuels”, J. of Nucl. Mater. **344**, 198-205 (2005).

Pu-U

K. Nakamura, M. Kurata, T. Ogata, T. Yokoo, and M. Mignanelli, “Phase relations in the Fe-Pu-U ternary system”, J. of Phase Equil. **22** (3), 259-264 (2001).

T. Ogata, K. Nakamura, M. Kurata, T. Yokoo, and M. Mignanelli, “Reactions between U-Pu-Zr alloys and Fe at 923 K”, J. of Nucl. Sci. and Techn. **37** (3), 244-252 (2000).

M. Kurata, “Thermodynamic assessment of the Pu-U, Pu-Zr, and Pu-U-Zr systems”, CALPHAD **23** (3-4), 305-337 (1999).

Yoshihiro Okamoto, Atsushi Maeda, Yasufumi Suzuki and Toshihiko Ohmichi, “Investigation of the Pu-U phase diagram”, J. of Alloys and Compounds **213/214**, 372-374 (1994).

L. Leibowitz, E. Veleckis, R. A. Blomquist, and A. D. Pelton, “Solidus and liquidus temperatures in the Uranium-Plutonium-Zirconium system”, J. of Nucl. Mater. **154**, 145-153 (1988).

L. Leibowitz, and R. A. Blomquist, and A. D. Pelton, “Thermodynamic modeling of the phase equilibria of the plutonium-uranium system”, J. of Nucl. Mater. **184**, 59-64 (1991).

Arthur D. Pelton, “Thermodynamic modeling and phase equilibrium calculations in nuclear materials”, Pure & Appl. Chem. **69** (11), 2245-2252 (1997).

F. H. Ellinger, R. O. Elliott, and E. M. Cramer, “The plutonium-uranium system”, J. of Nucl. Mater. **3**, 233-243 (1959).

M. C. Petri, A. G. Hins, J. E. Sanecki, and M. A. Dayananda, “Uranium-plutonium interdiffusion at 750 °C”, J. of Nucl. Mater. **211**, 1-10 (1994).

Kosuke Tanaka, Koji Maeda, Kozo Katsuyama, Masaki Inoue, Takashi Iwai, Yasuo Arai, “Fission gas release and swelling in uranium-plutonium mixed nitride fuels”, J. of Nucl. Mater. **327**, 77-87 (2004).

J. I. Bramman, R. M. Sharpe, and R. Dixon, “Fission-product inclusions in irradiated uranium-plutonium carbide”, J. of Nucl. Mater. **38**, 226-229 (1971).

Pu-Zr

H. Kinoshita, M. Uno, and S. Yamanaka, “Phase relation assessment of the O-Pu-Zr system by thermodynamic modeling”, J. of Alloys and Compounds **353**, 129-137 (2003).

M. Kurata, “Thermodynamic assessment of the Pu-U, Pu-Zr, and Pu-U-Zr systems”, CALPHAD **23** (3-4), 305-337 (1999).

Yasufumi Suzuki, Atsushi Maeda and Toshihiko Ohmichi, “Phase diagram of the Pu-Zr system in the Zr-rich region”, J. of Alloys and Compounds **182**, L9-L14 (1992).

L. Leibowitz, E. Veleckis, R. A. Blomquist, and A. D. Pelton, “Solidus and liquidus temperatures in the Uranium-Plutonium-Zirconium system”, J. of Nucl. Mater. **154**, 145-153 (1988).

J. A. C. Maples, “The Plutonium-Zirconium phase diagram”, J. of the Less-Common Metals **2**, 331-351 (1960).

Si-U

Tristan Lebihan, Peter Rogl, and Henri Noël, “The Niobium-Silicon-Uranium system”, J. of Nucl. Mater. **277**, 82-90 (2000).

H. Vaugoyeau, L. Lombard, and J. P. Morlevat, “Contribution à l’étude du diagramme d’équilibre Uranium Silicium”, J. of Nucl. Mater. **39**, 323-329 (1971).

U-Zr

S. Dash, Z. Singh, T. R. G. Kutty, S. C. Parida, and V. Venugopal, “Thermodynamic studies on Al-U-Zr alloys”, J. of Alloys and Compounds **365**, 291-299 (2004).

K. Nakamura, M. Kurata, T. Ogata, A. Itoh, and M. Akabori, “Equilibrium phase relations in the U-Zr-Fe ternary system”, J. of Nucl. Mater. **275**, 151-157 (1999).

M. Kurata, T. Ogata, K. Nakamura, and T. Ogawa, “Thermodynamic assessment of the Fe-U, U-Zr and Fe-U-Zr systems”, J. of Alloys and Compounds **271-273**, 636-640 (1998).

P. Y. Chevalier, E. Fischer, and B. Cheynet, “Progress in the thermodynamic modeling of the O-U-Zr ternary system”, CALPHAD **28**, 15-40 (2004); and references therein.

L. Leibowitz, and R. A. Blomquist, and A. D. Pelton, “Thermodynamics of the uranium-zirconium system”, J. of Nucl. Mater. **167**, 76-81 (1989).

P. Y. Chevalier and E. Fischer, “Thermodynamic modelling of the O-U-Zr system”, J. of Nucl. Mater. **257**, 213-255 (1998).

T. Ogata, K. Nakamura, M. Kurata, T. Yokoo, and M. Mignanelli, “Reactions between U-Pu-Zr alloys and Fe at 923 K”, J. of Nucl. Sci. and Techn. **37** (3), 244-252 (2000).

M. Kurata, “Thermodynamic assessment of the Pu-U, Pu-Zr, and Pu-U-Zr systems”, CALPHAD **23** (3-4), 305-337 (1999).

Masaki Kurata, Takanari Ogata, Kinya Nakamura, Toru Ogawa, “Thermodynamic assessment of the Fe-U, U-Zr and Fe-U-Zr systems”, J. of Alloys and Compounds **271-273**, 636-640 (1998).

L. Leibowitz, E. Veleckis, R. A. Blomquist, and A. D. Pelton, “Solidus and liquidus temperatures in the Uranium-Plutonium-Zirconium system”, J. of Nucl. Mater. **154**, 145-153 (1988).

A. D. Pelton, P. K. Talley, L. Leibowitz, and R. A. Blomquist, “Thermodynamic analysis of phase equilibria in the iron-uranium-zirconium system”, J. of Nucl. Mater. **210**, 324-332 (1994).

G. L. Hofman, S. L. Hayes, and M. C. Petri, “Temperature gradient driven constituent redistribution in U-Zr alloys”, J. of Nucl. Mater. **227**, 277-286 (1996).

Byung-Ho Lee, Jin-Sik Cheon, Yang-Hyun Koo, Je-Yong Oh, Jeong-Sik Yim, Dong-Seong Sohn, M. Baryshnikov, A. Gaiduchenko, “Measurement of the specific heat of Zr-40 wt% U metallic fuel”, J. of Nucl. Mater. **360**, 315-320 (2007).

J. Rest, “Kinetics of fission-gas-bubble-nucleated void swelling of the alpha-uranium phase of irradiated U-Zr and U-Pu-Zr fuel”, J. of Nucl. Mater. **207**, 192-204 (1993).

T. Ogawa, T. Iwai, and M. Kurata, “Demixing of U-Zr alloys under a thermal gradient”, J. of the Less Com. Met. **175**, 59-69 (1991).

T. Ogawa and T. Iwai, “Thermochemical modelling of U-Zr alloys”, J. of the Less Com. Met. **170**, 101-108 (1991).

Tsuneo Matsui, Tetsuya Natsume, and Keiji Naito, “Heat capacity measurements of $U_{0.80}Zr_{0.20}$ and $U_{0.80}Mo_{0.20}$ alloys from room temperature to 1300 K”, J. of Nucl. Mater. **167**, 152-159 (1989).

L. V. Pavlinov, A. I. Nakonechniko, and V. N. Bykov, “Diffusion of uranium in molybdenum, niobium, zirconium and titanium”, J. of Nucl. Mater. **20**, 1027-1030 (1966).

T. Ogawa, T. Ogata, A. Itoh, M. Akabori, H. Miyanishi, H. Sekino, M. Nishi, and A. Ishikawa, “Irradiation behavior of microspheres of U-Zr alloys”, J. of Alloys and Compounds **271-273**, 670-675 (1998).

M. Akabori, A. Itoh, T. Ogawa, and T. Ogata, “Interdiffusion in the U-Zr system at δ -phase

compositions”, J. of Alloys and Compounds **271–273**, 597–601 (1998).

Mitsuo Akabori, Toru Ogawa, Akinori Itoh, and Yukio Morii, “The lattice stability and structure of δ -UZr₂ at elevated temperatures”, J. of Phys.: Condens. Mater. **7**, 8249-8257 (1995).

Toru Ogawa, J. K. Gibson, R. G. Haire, M. M. Gensini, and M. Akabori, “Thermodynamic analysis of Zr-U and Zr-Np alloys in view of f-d interaction”, J. of Nucl. Mater. **223**, 67-71 (1995).

K. Nagarajan, R. Babu, and C. K. Mathews, “Enthalpy of formation of UZr₂ by calorimetry”, J. of Nucl. Mater. **203**, 221-223 (1993).

M. Akabori, A. Itoh, T. Ogawa, F. Kobayashi, and Y. Suzuki, “Stability and structure of the δ phase of the U-Zr alloys”, J. of Nucl. Mater. **188**, 249-254 (1992).

Yoichi Takahashi, Michio Yamawaki, and Kazutaka Yamamoto, “Thermophysical Properties of Uranium-Zirconium Alloys”, J. of Nucl. Mater. **154**, 141-144 (1988).

Atsushi Maeda, Yasufumi Suzuki, and Toshihiko Ohmichi, “Uranium activity of uranium-rich U-Zr alloys by Knudsen effusion mass spectrometry”, J. of Alloys and Compounds **179**, L21-24 (1992).

Masayoshi Kanno, Michio Yamawaki, Tadafumi Koyama, and Nobuo Morioka, “Thermodynamic Activity Measurements of U-Zr Alloys by Knudsen Effusion Mass Spectrometry”, J. of Nucl. Mater. **154**, 154-160 (1988).

References – Other Binaries of Interest

Am-Np

J. K. Gibson and R. G. Haire, “Phase relations in neptunium, americium, and the binary alloy systems Np-Am and Np-Ln (Ln=La, Nd, Lu), J. of Nucl Mater. **195**, 156-165 (1992).

J. K. Gibson, R. G. Haire, M. M. Gensini, and T. Ogawa, “Alloying behavior in selected neptunium binary systems: the role of 5f bonding”, J. of Alloys and Compounds **213/214**, 106-110 (1994).

H. Okamoto, “Am-Np (Americium-Neptunium)”, J. of Phase Equilibria **20** (4), 450 (1999).

Am-Pu

F. H. Ellinger, K. A. Johnson, and V. O. Struebing, “The Plutonium-Americium system”, J. of Nucl. Mater. **20**, 83-86 (1966).

V. D. Shumakov, N. S. Kosulin, and N. T. Chebotarev, “Phase diagram of Plutonium-Americium alloys” (1990), UDC 669.018.824.

A. Shick, L. Havela, J. Kolorenc, V. Drchal, T. Gouder, and P. Oppeneer, “Electronic structure and nonmagnetic character of δ -Pu-Am alloys”, Phys. Rev. B **73**, 104415-1 to 4 (2006).

N. Baclet, M. Dormeal, L. Havela, J. M. Fourier, C. Valot, F. Wastin, T. Gouder, E. Colineau, C. T. Walker, S. Bremier, C. Apostolidis, and G. H. Lander, “Character of 5f states in the Pu-Am system from magnetic susceptibility, electrical resistivity, and photoelectron spectroscopy measurements”, Phys. Rev. B **75**, 035101-1 to 9 (2007).

Am-X

“Phase equilibria, crystallographic and thermodynamic data for binary alloys”, Landolt-Börnstein, New Series IV/12A, Supplement to IV/5A. (Am-X_Refs, LB_Actinide Alloys.pdf).

B-Zr

H. M. Chen, F. Zheng, H. S. Liu, L. B. Liu, and Z. P. Jin, “Thermodynamic assessment of B-Zr and Si-Zr binary systems”, J. of alloys and Compounds (2008). (doi:10.1016/j.jallcom.2008.01.061).

C-Si

Joachim Gröbner, Hans Leo Lukas, and Fritz Aldinger, “Thermodynamic calculation of the ternary system Al-Si-C”, CALPHAD **20** (20), 247-254 (1996).

C-Zr

A. Fernandez Guillermet, “Analysis of thermochemical properties and phase stability in the zirconium-carbon system”, J. of Alloys and Compounds **217**, 69-89, 1995.

M. Jiang, K. Oikawa, T. Ikeshoji, L. Wulff, and K. Ishida, “Thermodynamic calculations of Fe-Zr and Fe-Zr-C systems”, J. of Phase Equil. **22** (4), 406-417 (2001).

H. M. Chen, Y. Xiang, S. Wang, F. Zheng, L. B. Liu, and Z. P. Jin, “Thermodynamic assessment of the C-Si-Zr system”, J. of Alloys and Compounds (2008) (doi:10.1016/j.jallcom.2008.06.086).

N-U

P. Y. Chevalier, E. Fischer, and B. Cheynet, “Thermodynamic modeling of the N-U system”, J. of Nucl. Mater. **280**, 136-150 (2000).

Np-O

Tsuyoshi Nishi, Akinori Itoh, Masahide Takano, Masami Numata, Mitsuo Akabori, Yasuo Arai, and Kazuo Minato, “Thermal conductivity of neptunium dioxide”, J. of Nucl. Mater. **376**, 78-82 (2008).

V. Sobolev, “Modelling thermal properties of actinide dioxide fuels”, J. of Nucl. Mater. **344**, 198-205 (2005).

Np-Pu

P. G. Mardon, J. H. Pearce, and J. A. C. Marples, “Constitution studies of the Neptunium-Plutonium alloy system”, J. of the Less Com. Met. **3**, 281-292 (1961).

Np-U

P. G. Mardon and J. H. Pearce, “An investigation of the neptunium-uranium equilibrium diagram”, J. of the Less Common Metals **1**, 467-475 (1959)

Np-Zr

R. Julian Rodriguez, C. Sari, and A. J. Criado Portal, “Investigation of the Np-Zr and U-Zr-Np systems”, J. of Alloys and Compounds **209**, 263-268 (1994).

J. K. Gibson and R. G. Haire, “Investigation of the neptunium-zirconium phase diagram by differential thermal analysis”, J. of Nucl. Mater. **201**, 225-230 (1993).

Toru Ogawa, J. K. Gibson, R. G. Haire, M. M. Gensini, and M. Akabori, “Thermodynamic analysis of Zr-U and Zr-Np alloys in view of f-d interaction”, J. of Nucl. Mater. **223**, 67-71 (1995).

Michel M. Gensini, Richard G. Haire, and John K. Gibson, “Investigation of the neptunium-zirconium system by X-ray diffraction”, J. of Alloys and Compounds **213/214**, 402-405 (1994).

J. K. Gibson, R. G. Haire, M. M. Gensini, and T. Ogawa, “Alloying behavior in selected

neptunium binary systems: the role of 5f bonding”, J. of Alloys and Compounds **213/214**, 106-110 (1994).

O-Th

F.N. Skomurski, L.C. Shuller, R.C. Ewing, and U. Becker, “Corrosion of UO₂ and ThO₂: A quantum-mechanical investigation”, J. of Nucl. Mater. **375**, 290-310 (2008).

V. Sobolev, “Modelling thermal properties of actinide dioxide fuels”, J. of Nucl. Mater. **344**, 198-205 (2005).

O-Zr

M. Barrachin, P.Y. Chevalier, B. Cheynet, and E. Fischer, “New modelling of the U-O-Zr phase diagram in the hyperstoichiometric region and consequences for the fuel rod liquefaction in oxidising conditions”, J. of Nucl. Mater. 2008.

C. Wang, M. Zinkevich, and F. Aldinger, “On the thermodynamic modeling of the Zr-O system”, CALPHAD **28**, 281-292 (2004).

H. Kinoshita, M. Uno, and S. Yamanaka, “Phase relation assessment of the O-Pu-Zr system by thermodynamic modeling”, J. of Alloys and Compounds **353**, 129-137 (2003).

P. Y. Chevalier, E. Fischer, and B. Cheynet, “Progress in the thermodynamic modeling of the O-U-Zr ternary system”, CALPHAD **28**, 15-40 (2004); and references therein.

P. Y. Chevalier and E. Fischer, “Thermodynamic modelling of the O-U-Zr system”, J. of Nucl. Mater. **257**, 213-255 (1998).

Pd-Si

R. Massara and P. Feschotte, “Le système binaire Pd-Si”, J. of alloys and Compounds **199**, 249-254 (1993).

Zhenmin Du, Cuiping Guo, Xiaojian Tang, and Ting Liu, “Thermodynamic description of the Pd-Si-C system”, Intermetallics **14**, 560-569 (2006).

Pd-Zr

Cuiping Guo, Zhenmin Du, and Changrong Li, “Thermodynamic modeling of the Pd-Zr system”, CALPHAD **30**, 482-488 (2006).

Si-Zr

H. M. Chen, F. Zheng, H. S. Liu, L. B. Liu, and Z. P. Jin, “Thermodynamic assessment of B-Zr and Si-Zr binary systems”, J. of alloys and Compounds (2008). (doi:10.1016/j.jallcom.2008.01.061).

H. M. Chen, Y. Xiang, S. Wang, F. Zheng, L. B. Liu, and Z. P. Jin, “Thermodynamic assessment of the C-Si-Zr system”, J. of Alloys and Compounds (2008) (doi:10.1016/j.jallcom.2008.06.086).

C. Guéneau, C. Servant, I. Ansara, and N. Dupin, “Thermodynamic assessment of the Si-Zr system”, CALPHAD **18** (3), 319-327 (1994).

References – Ternaries and Higher-Order Component Alloys

Am-O-Pu

M. Osaka, K. Kurosaki, and S. Yamanaka, “Oxygen potential of $(\text{Pu}_{0.91}\text{Am}_{0.09})\text{O}_{2-x}$ ”, J. of Nucl. Mater. **357**, 69-76 (2006).

M. Osaka, K. Kurosaki, and S. Yamanaka, “Chemical thermodynamic analysis of americium-containing UO_2 and $(\text{U,Pu})\text{O}_2$ ”, J. of Alloys and Compounds **428**, 355-361 (2007).

Shuhei Miwa, Masahiko Osaka, Hiroshi Yoshimochi, Kenya Tanaka, Ken Kurosaki, Masayoshi Uno, and Shinsuke Yamanaka, “Phase behavior of PuO_{2-x} with addition of 9% Am”, J. of Alloys and Compounds **444-445**, 610-613 (2007).

Am-O-Pu-U

Masahiko Osaka, Takashi Namekawa, Ken Kurosaki, and Shinsuke Yamanaka, “Chemical thermodynamic representation of $(\text{U,Pu,Am})\text{O}_{2-x}$ ”, J. of Nucl. Mater. **344**, 230-234 (2005).

Kyoichi Morimoto, Masato Kato, Masahiro Ogasawara, Motoaki Kashimura, Tomoyuki Abe, “Thermal conductivities of $(\text{U,Pu,Am})\text{O}_2$ solid solutions”, J. of Alloys and Compounds **452**, 54-60 (2008).

C-Pd-Si

Zhenmin Du, Cuiping Guo, Xiaojian Tang, and Ting Liu, “Thermodynamic description of the Pd-Si-C system”, *Intermetallics* **14**, 560-569 (2006).

Karanam Bhanumurthy and Rainer Schmid-Fetzer, “Experimental Study of ternary Pd-Si-C phase equilibria and Pd/SiC interface reactions”, *Z. Metallkd.* **87** (4), 244-253 (1996).

C-O-U

A. Pialoux and M. Dode, “Contribution a l’établissement du diagramme de phases du système U-C-O à l’aide de la diffractométrie de rayons X à haute temperature sous pression contrôlée”, *J. of Nucl. Mater.* **56**, 221-228 (1975).

N. A. Javed, “Phase relations in the uranium-carbon-oxygen system at 1573 K”, *J. of Nucl. Mater.* **37**, 353-354 (1970).

C-Si-Zr

H. M. Chen, Y. Xiang, S. Wang, F. Zheng, L. B. Liu, and Z. P. Jin, “Thermodynamic assessment of the C-Si-Zr system”, *J. of Alloys and Compounds* (2008) (doi:10.1016/j.jallcom.2008.06.086).

K. Bhanumurthy and R. Schmid-Fetzer, “Interface reactions between SiC/Zr and development of zirconium base composites by in situ solid state reactions”, *Scripta Mater.* **45**, 547-553 (2001).

M-O-Zr

Hajime Kinoshita, Masayoshi Uno, and Shinsuke Yamanaka, “Stability evaluation of fluorite structure phases in ZrO_2 - MO_2 (M = Th, U, Pu, Ce) systems by thermodynamic modeling”, *J. of Alloys and Compounds* **370**, 25-30 (2004).

N-Pu-U

Kosuke Tanaka, Koji Maeda Kozo Katsuyama, Masaki Inoue, Takashi Iwai, Yasuo Arai, “Fission gas release and swelling in uranium-plutonium mixed nitride fuels”, *J. of Nucl. Mater.* **327**, 77-87 (2004).

Toru Ogawa and Mitsuo Akabori, “Thermodynamic properties and multiphase diffusion paths of the ternary system U-Zr-N”, *J. of alloys and Compounds* **213/214**, 173-177 (1994).

Np-O-Pu-U

Masayuki Hirota, Ken Kurosaki, Daigo Setoyama, Masato Kato, Masahiko Osaka, Takashi Namekawa, Masayoshi Uno, and Shinsuke Yamanaka, “Thermodynamic modelling of the (U, Pu,Np)O_{2±x} mixed oxide”, J. of Nucl. Mater. **344**, 84-88 (2005).

Np-U-Zr

R. Julian Rodriguez, C. Sari, and A. J. Criado Portal, “Investigation of the Np-Zr and U-Zr-Np systems”, J. of Alloys and Compounds **209**, 263-268 (1994).

O-Pu-U

Theodore M. Besmann and Terrence B. Lindemer, “Chemical thermodynamic representations of <PuO_{2-x}> and <U_{1-z}Pu_zO_w>”, J. of Nucl. Mater. **130**, 489-504 (1985).

M. Kato, K. Morimoto, H. Sugata, K. Konashi, M. Kashimura, and T. Abe, “Solidus and liquidus temperatures in the UO₂–PuO₂ system”, J. of Nucl. Mater. **373**, 237-245 (2008).

Masato Kato, Kyoichi Morimoto, Hiromasa Sugata, Kenji Konashi, Motoaki Kashimura, and Tomoyuki Abe, “Solidus and liquidus of plutonium and uranium mixed oxide”, J. of Alloys and Compounds **452**, 48-53 (2008).

Heiko Kleykamp, “Phase equilibria in the UO₂-PuO₂ system under a temperature gradient”, J. of Nucl. Mater. **294**, 8-12 (2001).

M. Bober, C. Sari, and G. Schumacher, “Redistribution of Plutonium and Uranium in mixed (U,Pu) oxide fuel materials in a thermal gradient”, J. of Nucl. Mater. **39**, 265-284 (1971).

Tatsumi Arima, Sho Yamasaki, Kazuya Idemitsu, and Yaohiro Inagaki, “Equilibrium and nonequilibrium molecular dynamics simulations of heat conduction in uranium oxide and mixed uranium–plutonium oxide”, J. of Nucl. Mater. **376**, 139-145 (2008).

O-Pu-U-Zr

H. Kinoshita, M. Uno, and S. Yamanaka, “Stability evaluation of fluorite structure phase in PuO₂-UO₂-ZrO₂ system by thermodynamic modelling”, J. of Nucl. Mater. **334**, 90-96 (2004).

O-U-Zr

P. Y. Chevalier, E. Fischer, and B. Cheynet, “Progress in the thermodynamic modeling of the O-U-Zr ternary system”, CALPHAD **28**, 15-40 (2004); and references therein.

P. Y. Chevalier and E. Fischer, “Thermodynamic modelling of the O-U-Zr system”, J. of Nucl. Mater. **257**, 213-255 (1998).

M. Barrachin, P.Y. Chevalier, B. Cheynet, and E. Fischer, “New modelling of the U-O-Zr phase diagram in the hyperstoichiometric region and consequences for the fuel rod liquefaction in oxidising conditions”, J. of Nucl. Mater. **375**, 397-409 (2008).

Pu-U-Zr

T. Ogata, K. Nakamura, M. Kurata, T. Yokoo, and M. Mignanelli, “Reactions between U-Pu-Zr alloys and Fe at 923 K”, J. of Nucl. Sci. and Techn. **37** (3), 244-252 (2000).

M. Kurata, “Thermodynamic assessment of the Pu-U, Pu-Zr, and Pu-U-Zr systems”, CALPHAD **23** (3-4), 305-337 (1999).

L. Leibowitz, E. Veleckis, R. A. Blomquist, and A. D. Pelton, “Solidus and liquidus temperatures in the Uranium-Plutonium-Zirconium system”, J. of Nucl. Mater. **154**, 145-153 (1988).

D. R. O’Boyle and A. Dwight, “The Uranium-Plutonium-Zirconium ternary alloy systems”, Nucl. Metall. **17**, 720 (1970).

Yeon Soo Kim, S. L. Hayes, G. L. Hofman, and A. M. Yacout, “Modeling of constituent redistribution in U-Pu-Zr metallic fuel”, J. of Nucl. Mater. **359**, 17-28 (2006).

Yeon Soo Kim, G. L. Hofman, S. L. Hayes and Y. H. Sohn, “Constituent redistribution in U–Pu–Zr fuel during irradiation”, J. of Nucl. Mater. **327** (1), 27-36 (2004).

Y. H. Sohn, M. A. Dayananda, G. L. Hofman, R. V. Strain, and S. L. Hayes, “Analysis of constituent redistribution in the γ (bcc) U-Pu-Zr alloys under gradients of temperature and concentrations”, J. of Nucl. Mater. **279**, 317-329 (2000).

J. Rest, “Kinetics of fission-gas-bubble-nucleated void swelling of the alpha-uranium phase of irradiated U-Zr and U-Pu-Zr fuel”, J. of Nucl. Mater. **207**, 192-204 (1993).

M. Ishida, T. Ogata, and M. Kinoshita, “Constituent migration model for U-Pu-Zr metallic fast reactor fuel”, Nucl. Technol. **104**, 37-51 (1993).

M. Ishida, T. Ogata, and M. Kinoshita, “Constituent migration model for fast reactor U-Pu-Zr metallic fuel”, Trans. Am. Nucl. Soc. **63**, 177 (1991).

D. L. Porter, C. E. Lahm, and R. G. Pahl, “Fuel constituent redistribution during the early stages of U-Pu-Zr irradiation”, *Metall. Trans.* **A21**, 1871-1876 (1990).

C. L. Trybus, J. E. Sanecki, and S. P. Henslee, “Casting of metallic fuel containing minor actinide additions”, *J. of Nucl. Mater.* **204**, 50-55 (1993).

C. Sari, C. T. Walker, M. Kurata, and T. Inoue, “Interaction of U-Pu-Zr alloys containing minor actinides and rare earths with stainless steel”, *J. of Nucl. Mater.* **208**, 201-210 (1994).

M. Kurata, T. Inoue, and C. Sari, “Redistribution behavior of various constituents in U-Pu-Zr alloy and U-Pu-Zr alloy containing minor actinides and rare earths in a temperature gradient”, *J. of Nucl. Mater.* **208**, 144-158 (1994).

Siegfried S. Hecker and Marius Stan, “Plutonium metallic fuels for fast reactors”, to be published in *J. of Nucl. Mater.* (2007).

M. C. Petri and M. A. Dayananda, “Isothermal diffusion in uranium-plutonium-zirconium alloys”, *J. of Nucl. Mater.* **240**, 131-143 (1997).

D. C. Crawford, C. E. Lahm, H. Tsai, and R. G. Pahl, “Performance of U-Pu-Zr fuel cast into zirconium molds”, *J. of Nucl. Mater.* **204**, 157-164 (1993).

O. A. Alekseev, E. A. Smirnov, and A. A. Shmakov, “Interdiffusion in the bcc phase of U-Pu-Zr system”, *Atomic Energy* **84** (4), 260-266 (1998).

References – Miscellaneous

J. K. Gibson, R. G. Haire, and T. Ogawa, “Semi-empirical models of actinide alloys”, *J. of Nucl. Mater.* **273**, 139-145 (1999).

J. K. Gibson, R. G. Haire, and M. M. Gensini, “Alloying behavior in selected neptunium binary systems: the role of 5f bonding”, *J. of Alloys and Compounds* **213/214**, 106-110 (1994).

T. Ogawa, “Alloying behavior among U, Np, Pu, and Am predicted with the Brewer valence bond model”, *J. of Alloys and Compounds* **194**, 1-7 (1993).

K. S. Chan, J. K. Lee, and H. I. Aaronson, “Kaufman approach calculations of partial phase diagrams amongst Th, U, Np, and Pu”, *J. of Nucl. Mater.* **92**, 237-242 (1980).

V. Pirlet, “Overview of actinides (Np, Pu, Am) and Tc release from waste glasses: influence of solution composition”, J. of Nucl. Mater. **298**, 47-54 (2001).

Christophe Thiebaut, Nathalie Baclet, Brice Ravat, Pierre Giraud, and Pascale Julia, “Effect of radiation on bulk swelling of plutonium alloys”, J. of Nucl. Mater. **361**, 184-191 (2007).

Heiko Kleykamp , “Highlights of experimental thermodynamics in the field of nuclear fuel development”, J. of Nucl. Mater. **344**, 1-7 (2005).

M. V. Nevitt And S. T. Zegler, “Transformation temperatures and structures in Uranium-Fissium alloys”, J. of Nucl. Mater. **1**, 6-12 (1959).

O. L. Kruger, “Phase relations and Structures in Uranium-Plutonium-Fissium alloys?”, J. of Nucl. Mater. **19**, 29-41 (1966).

I. Grenthe, J. Fuger, R. J. M. Konings, R. J. Lemire, A. B. Muller, C. Nguyen-Trung Cregu, and H. Wanner, “Chemical Thermodynamics of Uranium”, edited by Hans Wanner and Isabelle Forest, OECD Nuclear Energy Agency, Data Bank, Issy-les Moulineaux (France), 2004 (735 pgaes).

C. Guéneau, S. Chatain, S. Gossé, C. Rado, O. Rapaud, J. Lechelle, J.C. Dumas, and C. Chatillon, “A thermodynamic approach for advanced fuels of gas-cooled reactors”, J. of Nucl. Mater. **344**, 191-197 (2005).